Supporting Information for

Transition Metal Mediated Nucleophilic Aromatic Substitution with Acids

Matthew E. O'Reilly,[†] Samantha Johnson,[‡] Robert J. Nielsen,[‡] William A. Goddard III*,[‡] and T. Brent Gunnoe[†]*

[†]*Department of Chemistry, University of Virginia, Charlottesville, Virginia 22904-4319, United States*
[‡]*Materials Process and Simulation Center, MC (139-74), California Institute of Technology, Pasadena, California 91125, United States*

Experimental

General Considerations. Unless otherwise noted, all synthetic procedures were performed under anaerobic conditions in a nitrogen filled glovebox or by using standard Schlenk techniques. Glovebox purity was maintained by periodic nitrogen purges and was monitored by an oxygen analyzer (O_2 < 15 ppm for all reactions). Tetrahydrofuran, pentane and diethyl ether were dried by distillation from sodium/benzophenone. Benzene, hexanes, and methylene chloride were purified by passage through a column of activated alumina. Benzene-d_6, chloroform-d_1, and tetrahydrofuran-d_8 were stored over 4Å molecular sieves in a nitrogen atmosphere. ^{1}H NMR spectra were recorded on a Varian Mercury Plus 300 MHz or a Varian Inova 500 MHz spectrometer, and the ^{13}C NMR spectra were recorded on a Varian Inova 500 MHz spectrometer (operating frequency 126 MHz). All ^{1}H and ^{13}C NMR spectra are referenced against residual proton signals (^{1}H NMR) or the ^{13}C resonances of the deuterated solvent (^{13}C NMR). $\{(COE)_2Rh(\mu\text{–}TFA)\}_2$ was prepared according to published literature procedures.[2] All other reagents were used as purchased from commercial sources.

Synthesis of 8,8'-(4,5-difluorobenzene)diquinoline (Q_2FB) (2). Quinolin-8-ylboronic acid (1.50 g, 8.67 x10^{-3} mol, 2.4 equiv.), 1,2-dibromo-4,5-difluorobenzene (0.985 g, 3.62 x10^{-3} mol, 1 equiv.), $Pd(PPh_3)_4$ (0.418 g, 3.62 x10^{-4} mol, 0.10 equivalents), and K_3PO_4 (17.0 g, 8.01 x10^{-2} mol, 22 equiv.) were combined into the 250 mL Schlenk flask. Under an inert atmosphere, degassed dimethylformaldehyde (60 mL) and degassed DI water (60 mL) were added to the Schlenk flask, and the flask was fitted with a glass stopper and sealed. The glass stopper was secured to the Schlenk flask with several rubber bands, and then the reaction mixture was heated in an oil bath at 110 °C with stirring for 14 h. Afterwards, the reaction mixture was allowed to cool to room temperature, during which the aqueous and organic layers separated. The lower aqueous phase was separated from the organic phase by separatory funnel and discarded. The organic layer was collected, and a copious amount of DI water (500 mL) was added to precipitate a yellow oily solid. The solid was collected by filtration and then dissolved in Et_2O (30 mL) and filtered. The filtrate was collected and reduced under mild pressure to an oil. The product was purified by column chromatography (silica). The mono-coupled product was removed as the first fraction using a solvent 1:10 (v/v) ethyl acetate:hexanes mixture, then the product was collected using ethyl acetate as an eluent. Evaporating the solvent in vacuo of the second fraction affords a yellow oily solid. The product was dried under vacuum for 2 days, triturated in pentane, and then filtered to obtain a white analytically pure **1** (0.229 g, Yield = 17%). ^{1}H NMR ($CDCl_3$, 600 MHz): δ = 8.81 (br, 2H, Ar–*H*), 8.00 (br, 2H, Ar–*H*), 7.54 (d, 2H, Ar–*H*, $^3J_{HH}$ = 8 Hz), 7.43 (t, 2H, Ar–*H*, $^3J_{HH}$ = 9 Hz), 7.28 (br, 4H, Ar–*H*), and 7.11 (br, 2H, Ar–*H*) ppm. ^{19}F NMR ($CDCl_3$, 600 MHz): δ = -140.6 (br, 2F) ppm. ^{13}C{^{1}H} NMR ($CDCl_3$, 150 MHz): δ = 150.2 (s, Ar–*C*), 149.2 (s, Ar–*C*, $^1J_{CF}$ = 249 Hz, $^2J_{CF}$ = 14 Hz), 146.5 (s, Ar–*C*), 139.2 (s, Ar–*C*), 136.3 (s, Ar–*C*), 136.0 (s, Ar–*C*), 131.2 (s, Ar–*C*), 128.2 (s, Ar–*C*), 127.5 (s, Ar–*C*), 125.6 (s, Ar–*C*), 120.9 (s, Ar–*C*), and 120.6 (s, Ar–*C*, $^2J_{CF}$ = 13 Hz, $^3J_{CF}$ = 6 Hz) ppm. Anal. Calcd. for $C_{24}H_{14}F_2N_2$ (368.39 g/mol): C: 78.25%; H: 3.83%; N: 7.70%, Found; C: 78.12%; H: 4.135%; N: 7.81%.

Synthesis of (Q_2FB)Rh(TFA)(COE) (3). A THF solution (5 mL) of ligand **2** (0.103 g, 2.80 x10^{-4} mol) was added to a THF solution (5 mL) of $\{Rh(\mu\text{–}TFA)(COE)_2\}_2$ (0.266 g, 6.1 x10^{-4} mol) dropwise and stirred for 0.5 h. The reaction mixture was dried under vacuum and the solid residue was washed with pentane (25 mL). The solid was dissolved in minimal THF (2 mL) and pentane (20 mL) was added to the solution to precipitate an orange powder. The solid was collected by filtration, washed with Et_2O (3x 5 mL), and dried under vacuum to afford the analytically pure **2** (0.135 g, yield = 69%). ^{1}H NMR (d_8-THF, 600 MHz): δ = 10.53-10.58 (s, 1H, Ar–*H*), 8.28 (s, 1H, Ar–*H*), 8.15 (br, 1H, Ar–*H*), 7.92-8.03 (br, 2H, Ar–*H*), 7.76-7.81 (s, 1H, Ar–*H*), 7.60 (br, 3H, Ar–*H*), 7.49 (d, 1H, Ar–*H*, $^3J_{HH}$ = 8 Hz), 6.88-7.01 (br, 3H, Ar–*H*), 6.75 (br, 1H, Ar–*H*), 5.51-5.59 (s, 1H, COE =C–*H*), 3.01-3.81 (br, 3H, COE-*H*), and 0.89-2.42 (m, COE-*H*) ppm. ^{19}F NMR (d_8-THF, 600 MHz): δ = -75.2 (br, TFA, minor isomer - 30%) and -74.4 (d, TFA, *J* = 6 Hz major isomer - 70%), -139.1 (m, Ar–*F*, minor isomer - 30%), -139.2 (m, Ar–*F*, major isomer - 70%), -140.0 (m, Ar–*F*, major isomer - 70%), and -140.3 (m, Ar–*F*, major isomer - 70%) ppm.

$^{13}C\{^1H\}$ NMR (d_8-THF, 150 HMz): δ = 157.7 (s, Ar–*C*), 157.5 (s, Ar–*C*), 156.5 (s, Ar–*C*), 152.2 (s, Ar–*C*), 150.5 (s, Ar–*C*), 140.5 (s, Ar–*C*), 139.6 (s, Ar–*C*), 137.1 (s, Ar–*C*), 136.4 (s, Ar–*C*), 134.5 (s, Ar–*C*), 133.8 (s, Ar–*C*), 132.1 (s, Ar–*C*), 130.8 (s, Ar–*C*), 129.7 (s, Ar–*C*), 129.4 (s, Ar–*C*), 129.1 (s, Ar–*C*), 128.4 (s, Ar–*C*), 128.3 (s, Ar–*C*), 128.1 (s, Ar–*C*), 126.5 (s, Ar–*C*), 126.4 (s, Ar–*C*), 122.6 (s, Ar–*C*), 122.4 (s, Ar–*C*), 122.3 (s, Ar–*C*), 121.6 (s, Ar–*C*), 121.4 (s, Ar–*C*), 121.3 (s, Ar–*C*), 118.7 (s, Ar–*C*), 118.6 (s, Ar–*C*), 68.4 (s, COE-*C*), 68.2 (s, COE-*C*), 68.1 (s, COE-*C*), 61.3 (s, COE-*C*), 61.1 (s, COE-*C*), 56.8 (s, COE-*C*), 56.7 (s, COE-*C*), 51.3 (s, COE-*C*), 51.2 (s, COE-*C*), 35.2 (s, COE-*C*), 31.1 (s, COE-*C*), 30.8 (s, COE-*C*), 30.2 (s, COE-*C*), 30.0 (s, COE-*C*), 29.3 (s, COE-*C*), 28.6 (s, COE-*C*), 27.8 (s, COE-*C*), 27.6 (s, COE-*C*), 27.5 (s, COE-*C*), 27.4 (s, COE-*C*), 27.2 (s, COE-*C*), 26.6 (s, COE-*C*), 26.4 (s, COE-*C*), 26.2 (s, COE-*C*), 26.0 (s, COE-*C*), 23.4 (s, COE-*C*), and 14.5 (s, COE-*C*) ppm. Anal. Calcd. for $C_{34}H_{28}F_5N_2O_2Rh$ (694.51 g/mol): C: 58.80%; H: 4.06%; N: 4.03%, Found; C: 58.62%; H: 3.97%; N: 3.81%.

Synthesis of $(Q_2FB)Rh(TFA)_3$ (1). Complex **3** (0.046 g, 6.62 x10^{-5} mol) was dissolved in THF (10 mL) and Ag(TFA) (0.031 g, 1.40 x10^{-4} mol) was added. The reaction mixture was stirred for 0.5 h turning from red to brown-yellow and depositing Ag(0). The reaction mixture was filtered, and the filtrate was reduced to a solid. The residue was washed with pentane before dissolving in minimal THF (1 mL) and precipitating the complex as a yellow-brown powder upon the addition of Et_2O (15 mL). Analytically pure **3** was isolated by filtration and dried under vacuum (0.026 g, 54%). ^1H NMR (*d*-THF, 600 MHz): δ = 9.23 (d, 2H, Ar–*H*, $^3J_{HH}$ = 5 Hz), 8.46 (d, 2H, Ar–*H*, $^3J_{HH}$ = 8 Hz), 7.86 (d, 2H, Ar–*H*, $^3J_{HH}$ = 8 Hz), 7.74 (t, 2H, Ar–*H*, $^3J_{HF}$ = 9 Hz), 7.69 (t, 2H, Ar–*H*, $^3J_{HH}$ = 6 Hz), 7.54 (t, 2H, Ar–*H*, $^3J_{HH}$ = 8 Hz), and 7.43 (d, 2H, Ar–*H*, $^3J_{HH}$ = 8 Hz) ppm. ^{19}F NMR (*d*-THF, 600 MHz): δ = -73.4 (s, 3F, TFA), -73.6 (s, 6F, TFA), and -124.9 (t, 2F, $^3J_{FH}$ = 9 Hz) ppm. $^{13}C\{^1H\}$ NMR ($CDCl_3$, 150 MHz): δ = 163.1 (q, O*C*(O)CF_3, $^1J_{CF}$ = 33 Hz), 160.9 (q, O*C*(O)CF_3, $^1J_{CF}$ = 40 Hz), 156.0 (dd, Ar–*C*, $^1J_{CF}$ = 249 Hz, $^2J_{CF}$ = 16 Hz), 155.5 (s, Ar–*C*), 152.8 (s, Ar–*C*), 141.7 (s, Ar–*C*), 134.9 (s, Ar–*C*), 134.5 (s, Ar–*C*), 128.8 (s, Ar–*C*), 127.0 (dd, Ar–*C*, $^2J_{CF}$ = 13 Hz, $^3J_{CF}$ = 6 Hz), 123.6 (s, Ar–*C*) and 123.0 (s, Ar–*C*) ppm. Anal. Calcd. for $C_{30}H_{14}F_{11}N_2O_6Rh$ (810.34 g/mol): C: 44.47%; H: 1.74%; N: 3.46%, Found; C: 44.46%; H: 1.90%; N: 3.41%.

Catalytic Defluorination. In a typical experiment, a J. Young tube was filled with 10 μL of fluoroarene, 5 mg of $[Cp^*Rh(C_6H_6)][BF_4]_2$ or 5 mg of $Ru(C_6H_6)Cl_2$/15 mg AgTFA, and 0.3 mL of HTFA. The contents were heated in an oil bath at 180 °C for 20 h prior to analysis by ^1H and ^{19}F NMR spectroscopy.

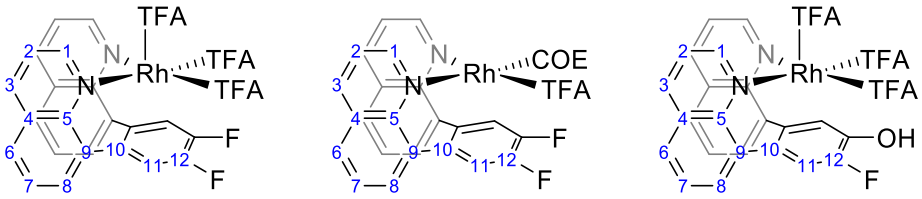

1 **3** **4**

Table S1. Assigned ^{1}H and ^{13}C chemical shifts for complexes **1**, **3**, and **4**.

	1		**3**		**4**	
Position	^{1}H	^{13}C	^{1}H	^{13}C	^{1}H	^{13}C
1	9.23	155.1	10.53	157.4	9.41	154.1
1'			8.25	156.1	9.14	153.7
2	7.69	123.6	7.57	122.3	7.80	122.8
2'			6.75	122.0	7.66	122.5
3	8.46	141.7	8.13	136.7	8.45	141.2
3'			7.81	136.0	8.40	141.5
4		130.4		129.5		130
4'				129.4		130
5		152.8		150.5		151.9
5'				152.3		151.1
6	7.85	130.5	7.49	127.9	7.88	129.5
6'			7.91	134.1	7.90	130.3
7	7.53	128.8	6.97	126.1	7.79	124.1
7'			7.57	127.9	7.57	128.2
8	7.44	134.4	6.95	131.7	7.36	134.3
8'			7.60	128.7	7.68	134.4
9		123.0		139.6		112.6
9'				140.5		124.5
10		134.4		133.8		142.5
10'				130.9		135.4
11	7.74	127.9	6.95	121.2	8.19	138.1
11'			7.99	118.2	8.25	133.4
12		156.0		152.2		159.2
12'				150.5		145.8
F		-121.9		-139.2		-108.9
F				-139.9		

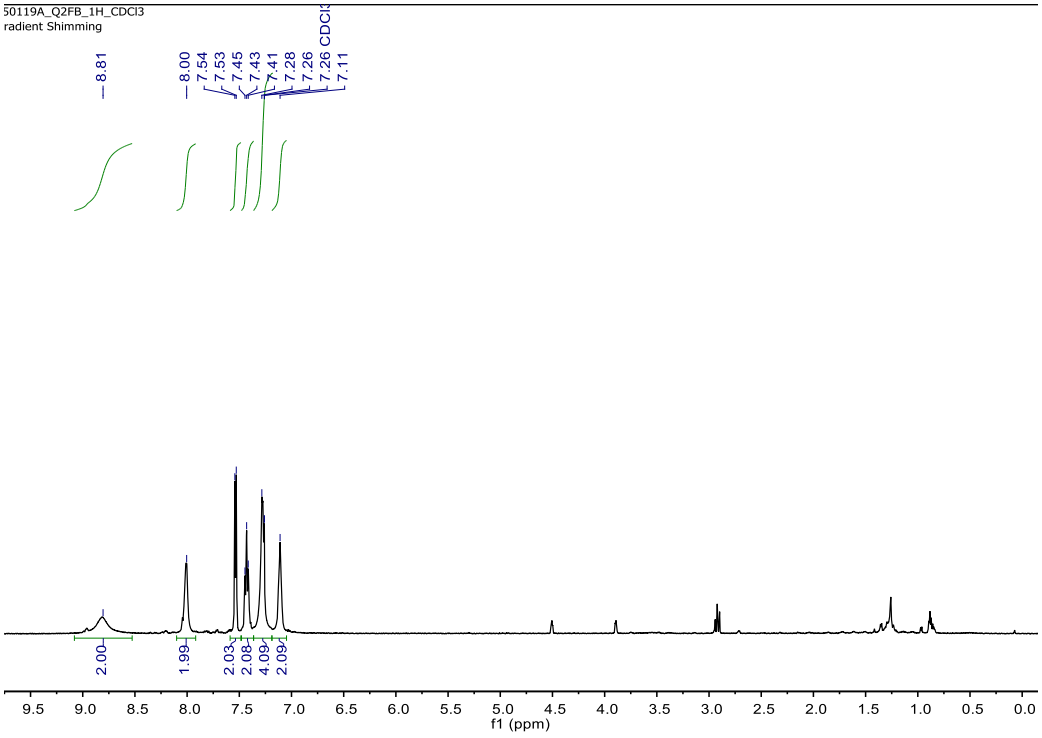

Figure S1. ^{1}H NMR spectrum (600 MHz, $CDCl_3$) of **2** (Q_2FB).

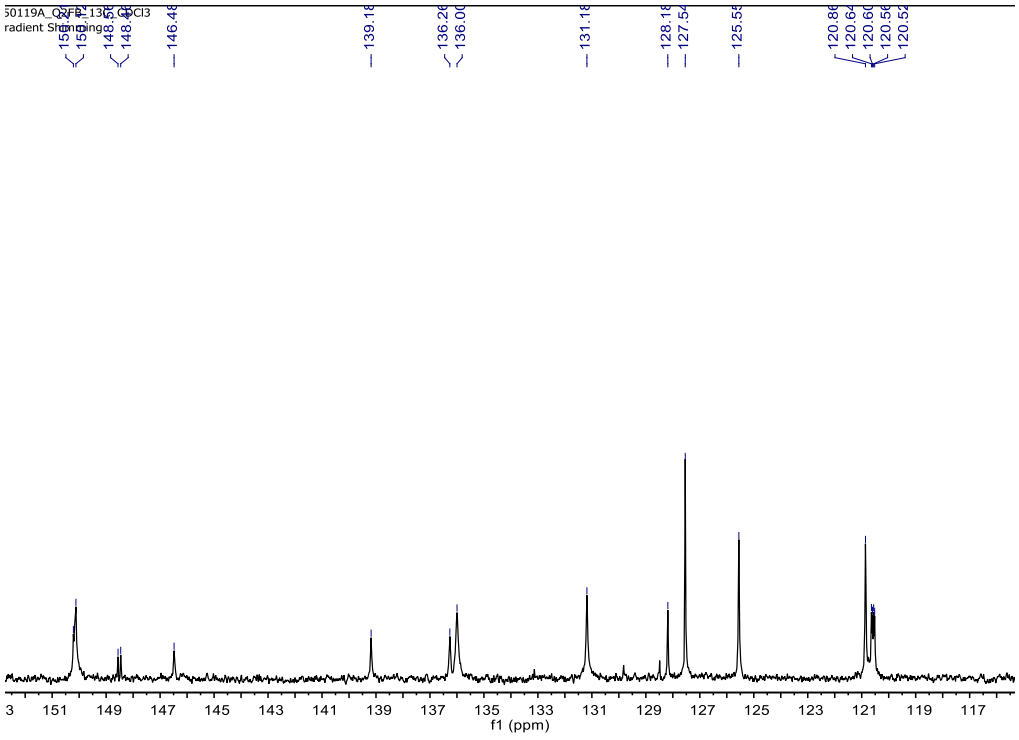

Figure S2. $^{13}C\{^{1}H\}$ NMR spectrum (150 MHz, $CDCl_3$) of **2** (Q_2FB).

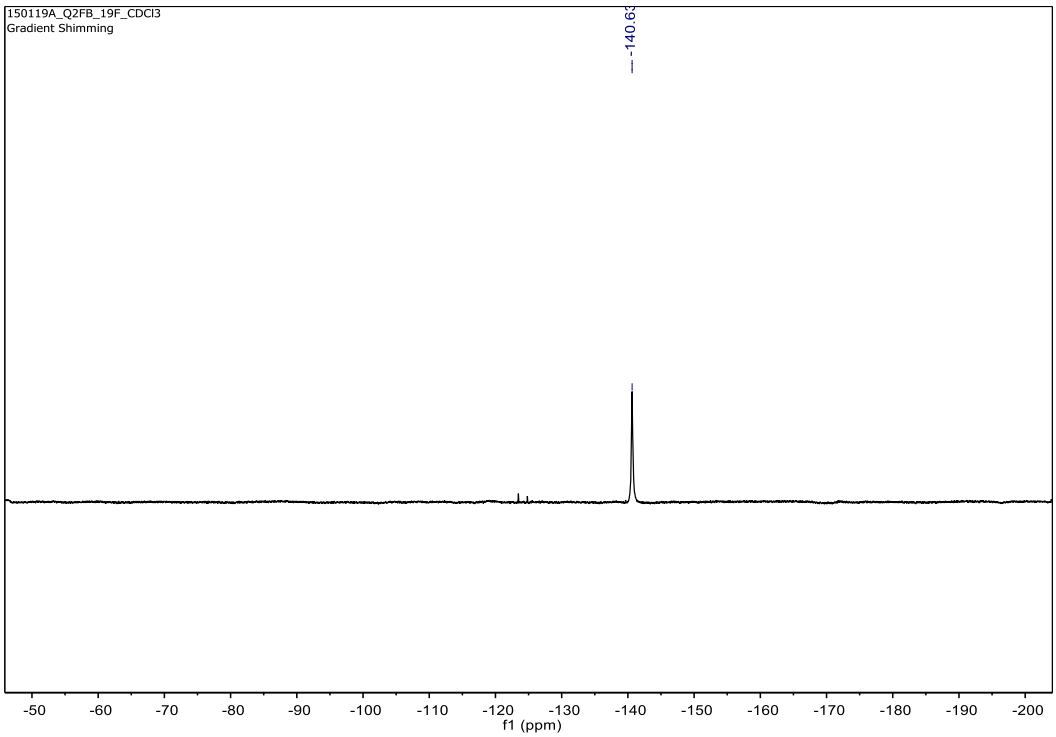

Figure S3. $^{19}F\{^{1}H\}$ NMR spectrum (600 MHz, $CDCl_3$) of **2** (Q_2FB).

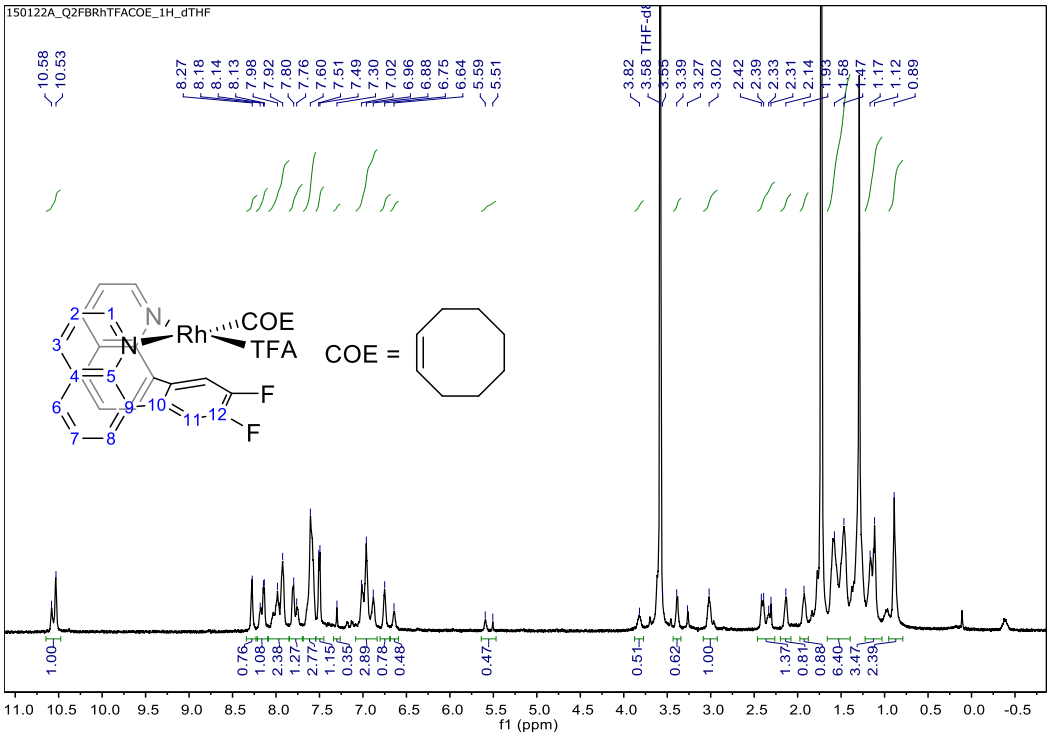

Figure S4. ^{1}H NMR spectrum (600 MHz, $CDCl_3$) of (Q_2FB)Rh(TFA)(COE) (**3**).

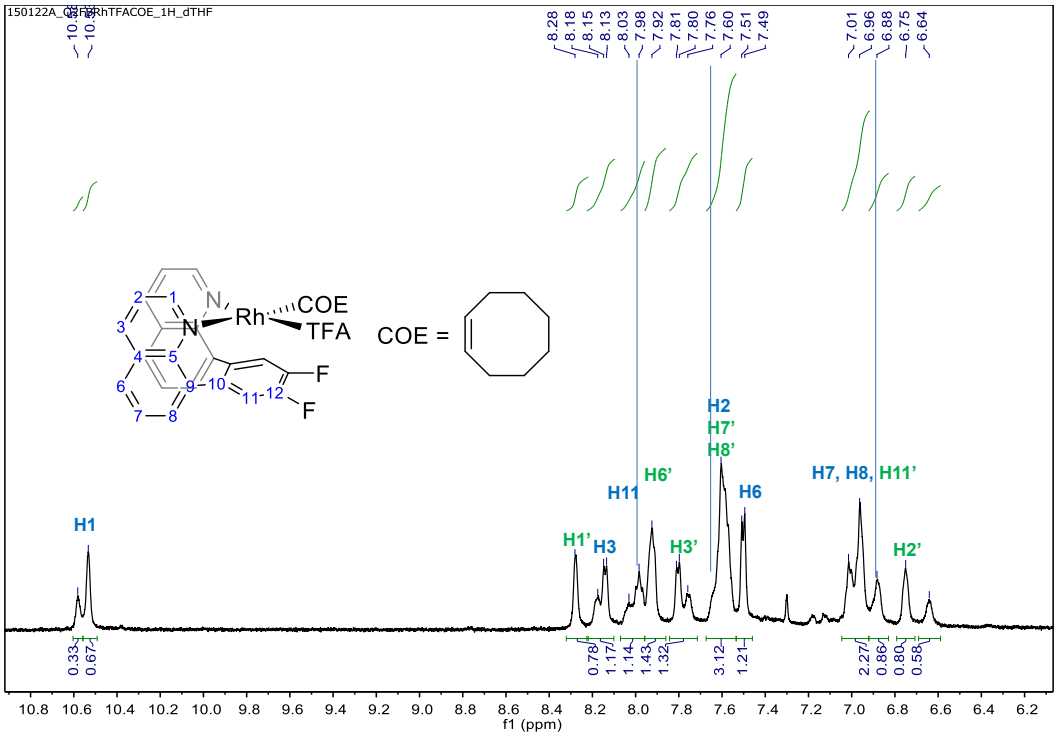

Figure S5. Expanded ^{1}H NMR spectrum (600 MHz, d_8-THF) of **3** (Q_2FB)Rh(TFA)(COE).

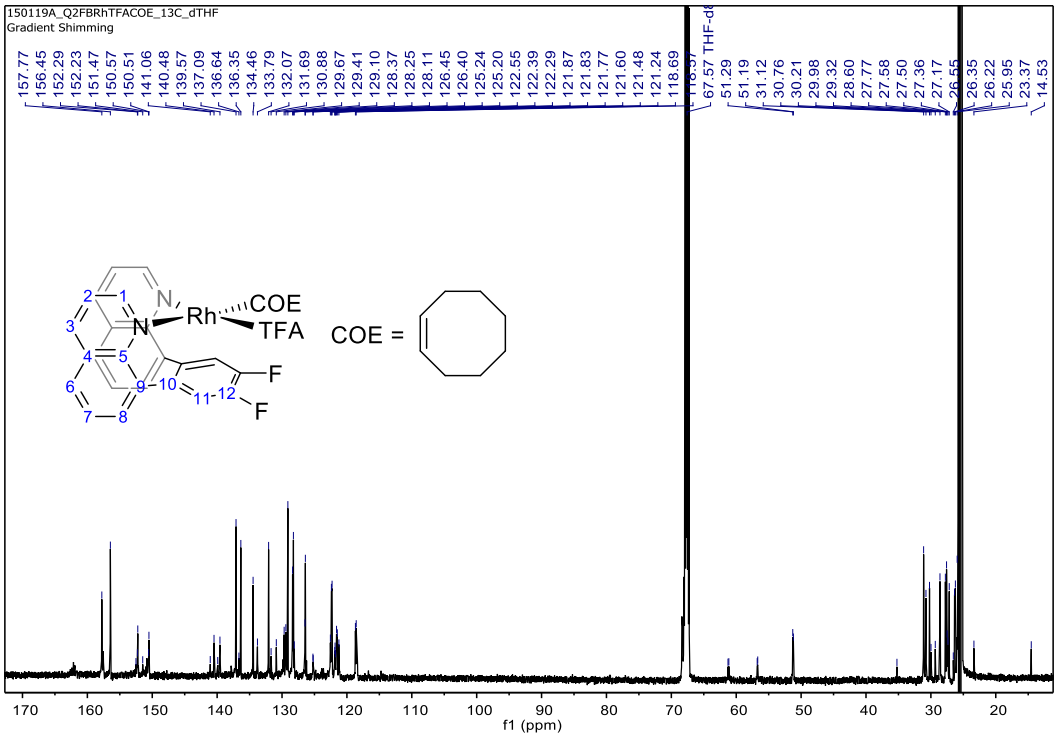

Figure S6. ^{13}C{^{1}H} NMR spectrum (150 MHz, d_8-THF) of **3** (Q_2FB)Rh(TFA)(COE).

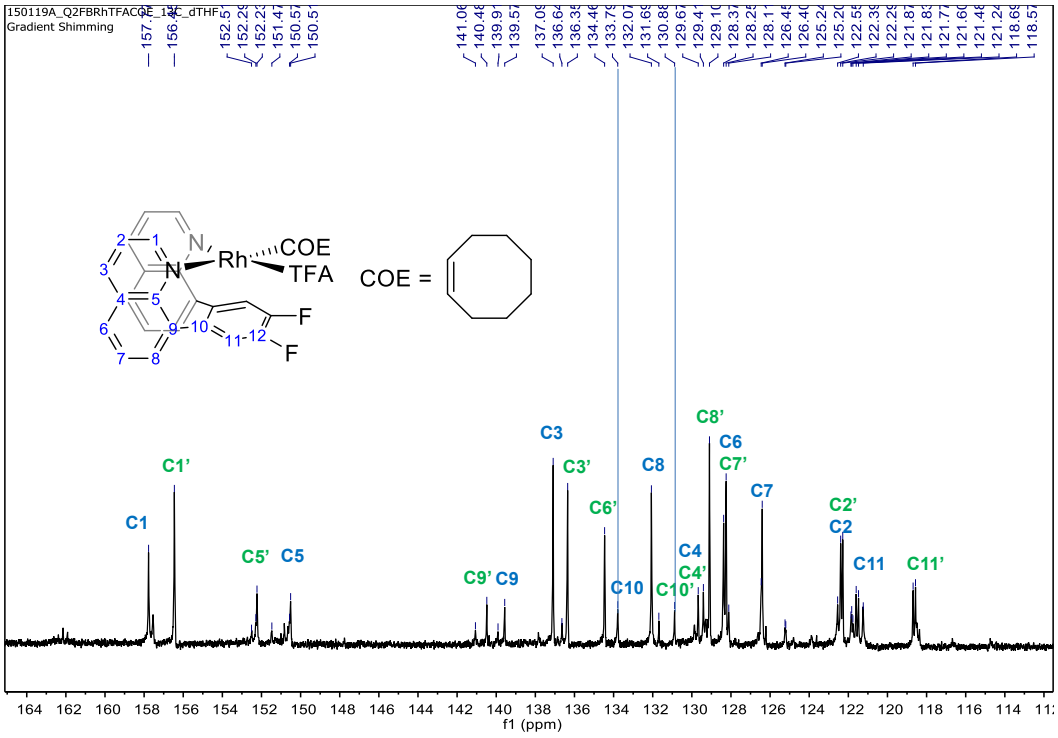

Figure S7. Expanded $^{13}C\{^{1}H\}$ NMR spectrum (150 MHz, d_8-THF) of **3** (Q_2FB)Rh(TFA)(COE).

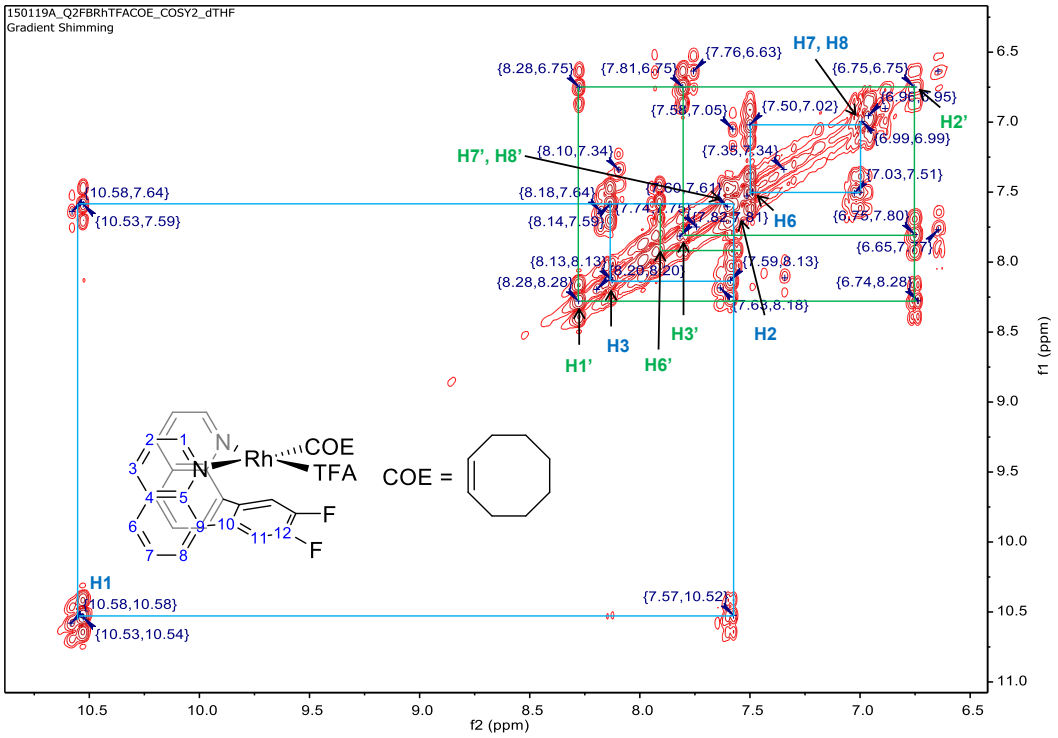

Figure S8. Expanded ^{1}H-^{1}H gCOSY NMR spectrum (600 MHz, d_8-THF) of **3** (Q_2FB)Rh(TFA)(COE).

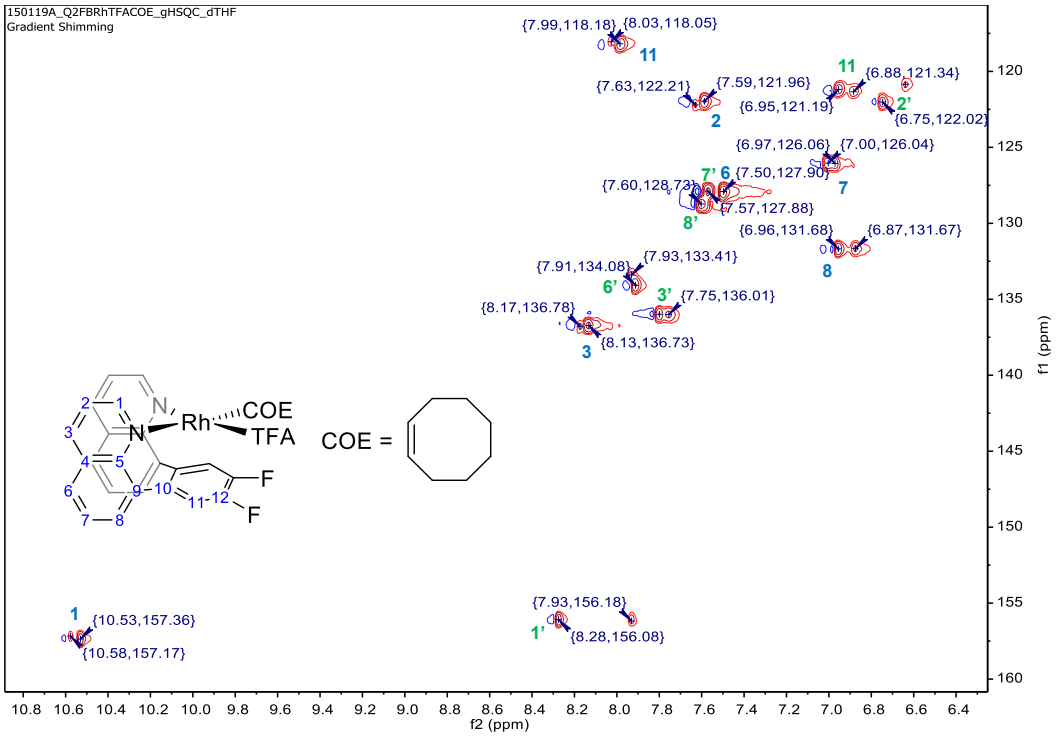

Figure S9. Expanded ^{1}H-^{13}C gHSQCAD NMR spectrum (600 MHz, d_8-THF) of **3** (Q_2FB)Rh(TFA)(COE).

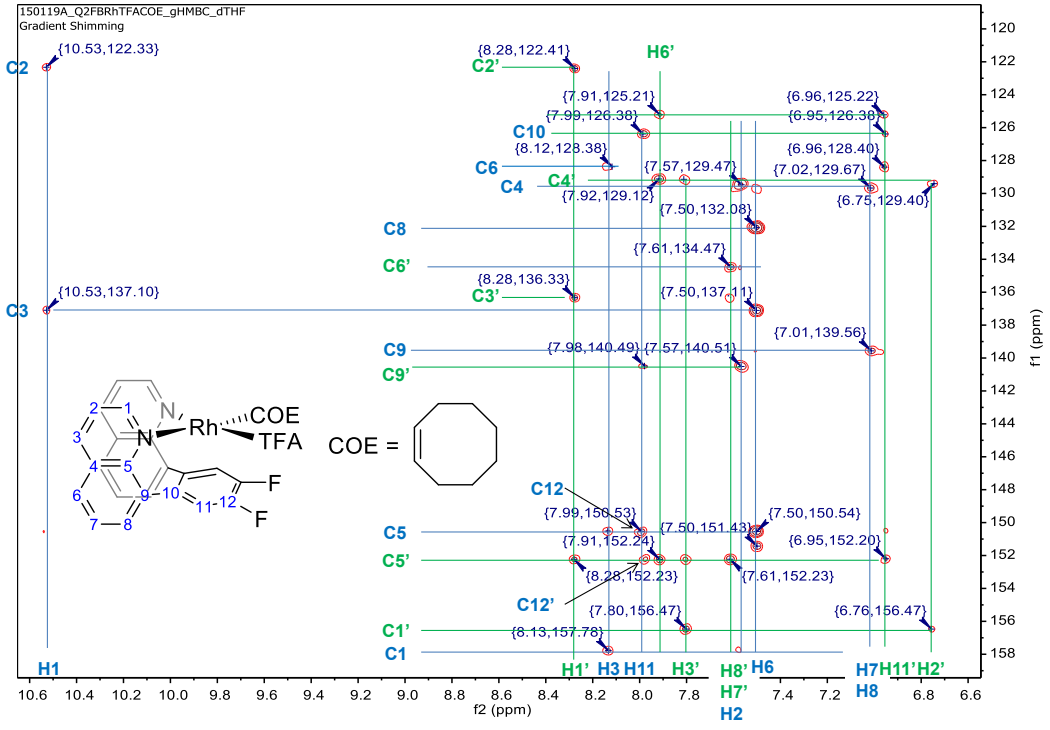

Figure S10. Expanded ^{1}H-^{13}C gHMBCAD NMR spectrum (600 MHz, d_8-THF) of **3** (Q_2FB)Rh(TFA)(COE).

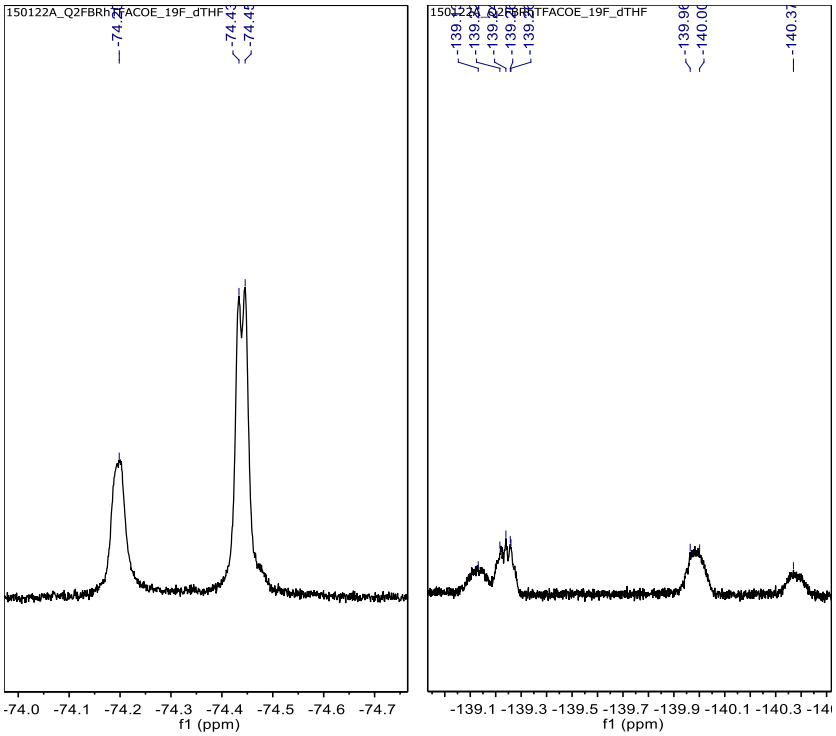

Figure S11. Expanded ^{19}F NMR spectrum (600 MHz, d_8-THF) of **3** (Q_2FB)Rh(TFA)(COE).

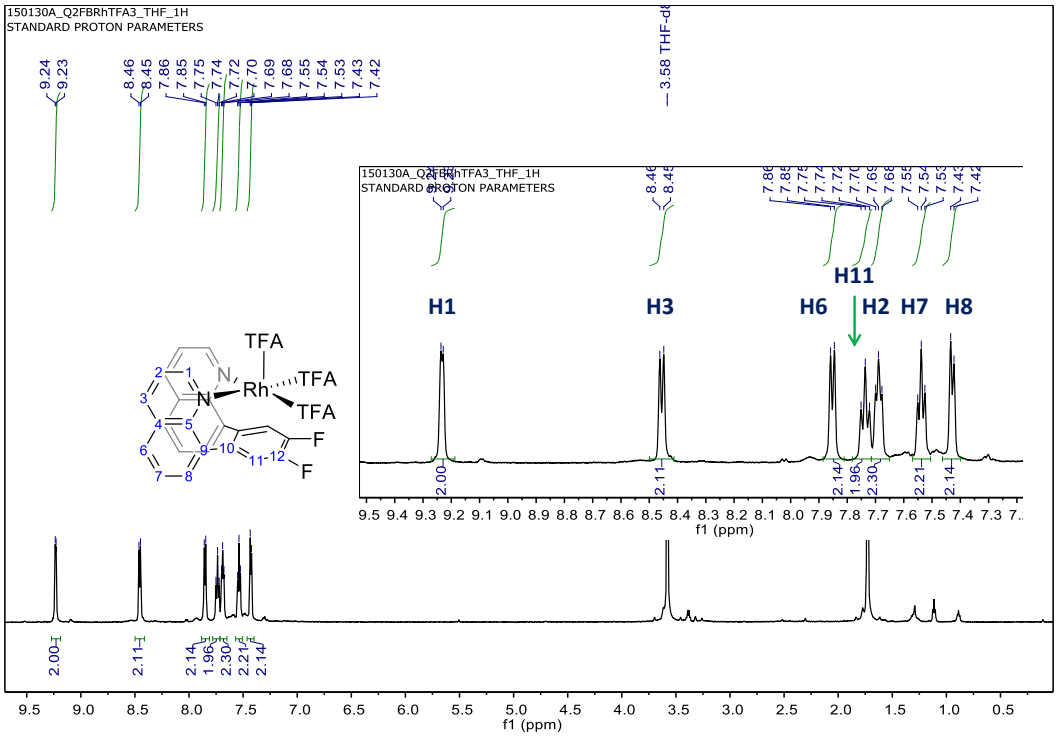

Figure S12. ^{1}H NMR spectrum (600 MHz, d_8-THF) of **1** (Q_2FB)Rh(TFA)$_3$.

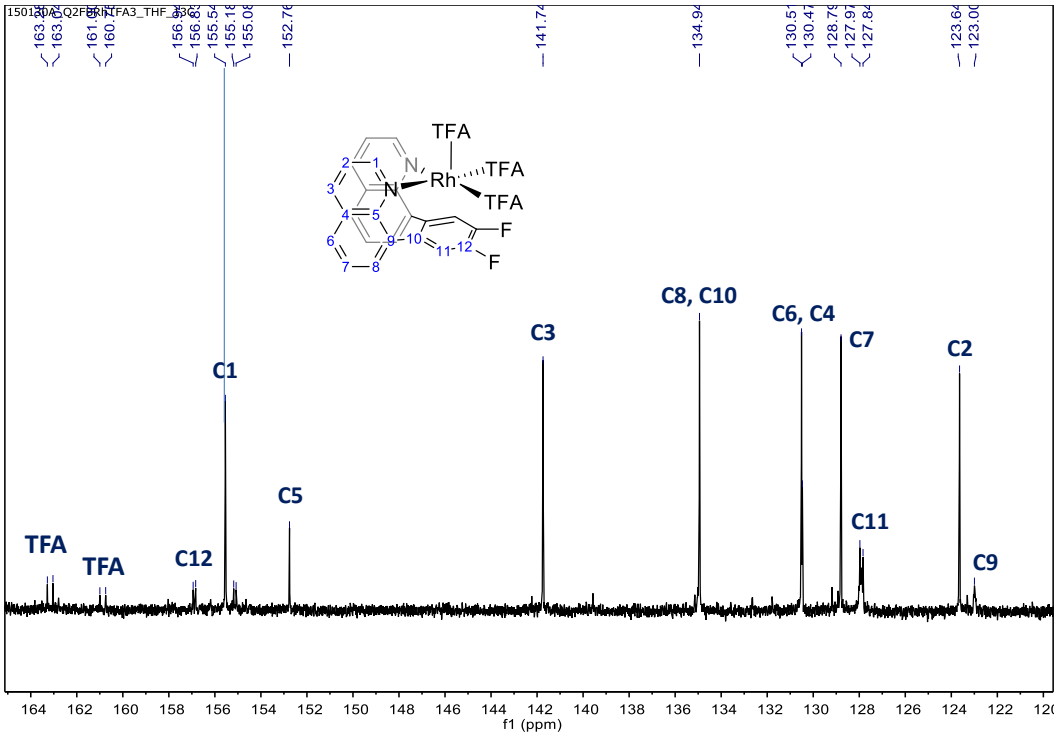

Figure S13. $^{13}C\{^{1}H\}$ NMR spectrum (150 MHz, d_8-THF) of **1** $(Q_2FB)Rh(TFA)_3$.

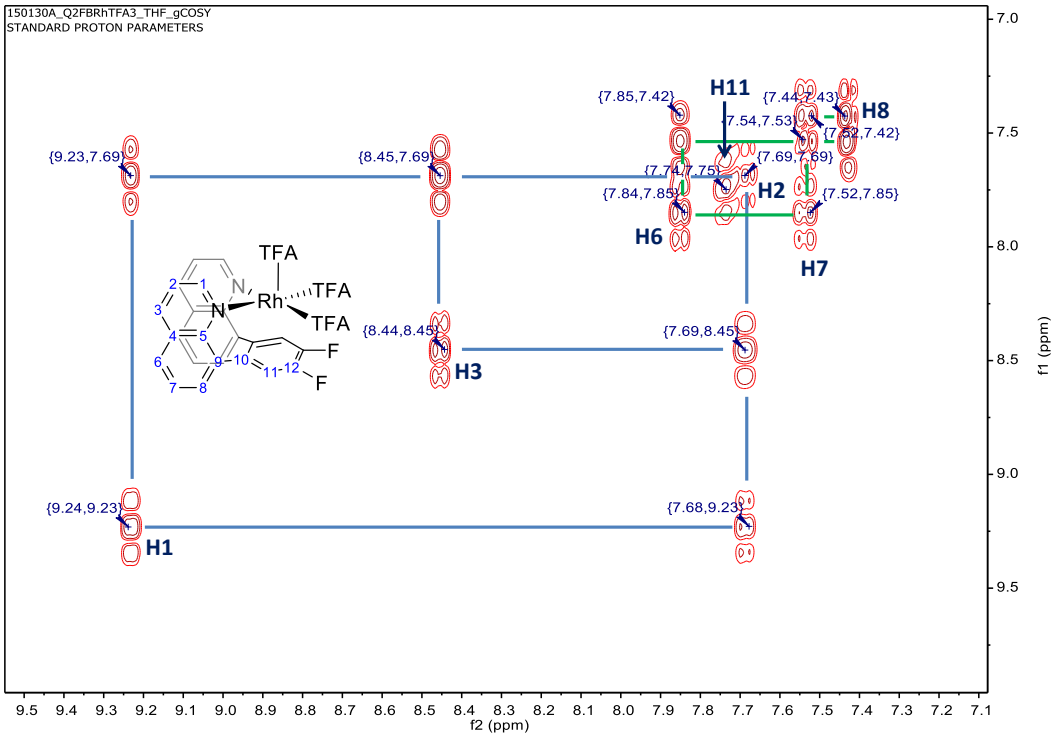

Figure S14. Expanded ^{1}H-^{1}H gCOSY NMR spectrum (600 MHz, d_8-THF) of **1** $(Q_2FB)Rh(TFA)_3$.

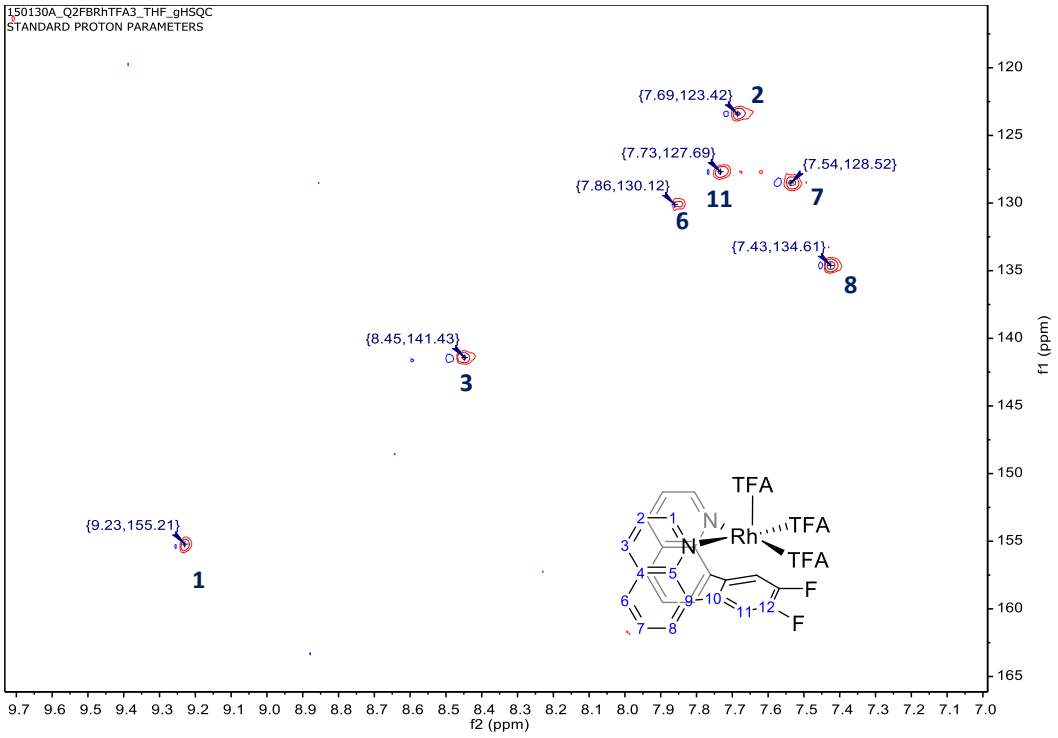

Figure S15. Expanded ^{1}H-^{13}C gHSQCAD NMR spectrum (600 MHz, d_8-THF) of **1** $(Q_2FB)Rh(TFA)_3$.

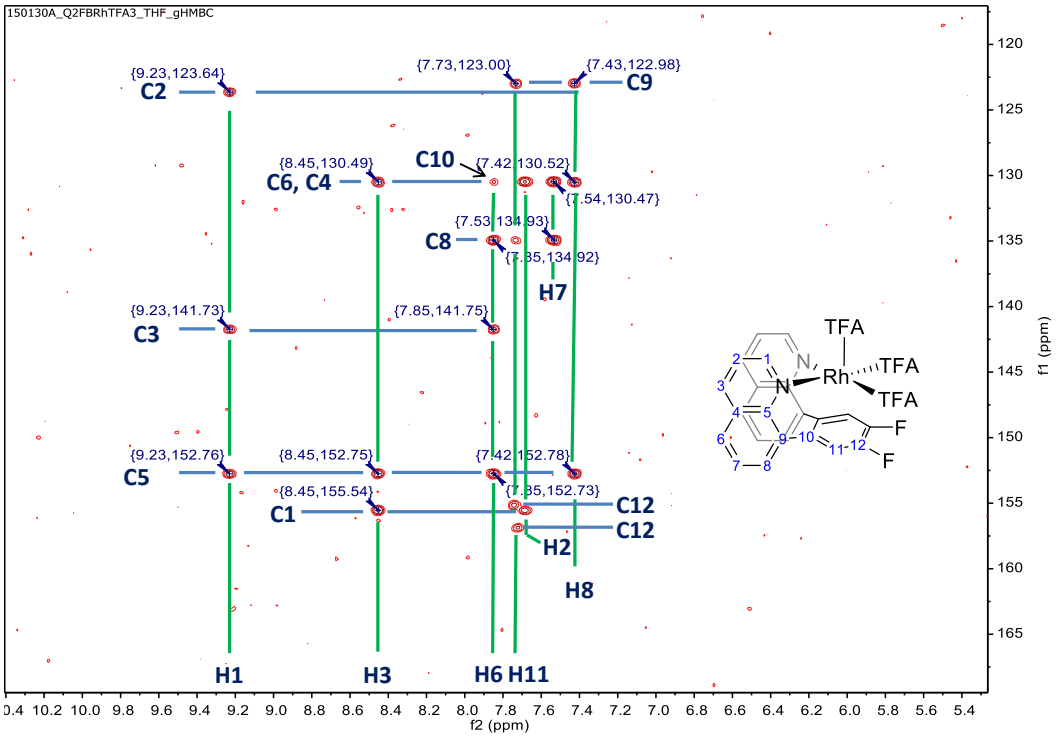

Figure S16. Expanded ^{1}H-^{13}C gHMBCAD NMR spectrum (600 MHz, d_8-THF) of **1** $(Q_2FB)Rh(TFA)_3$.

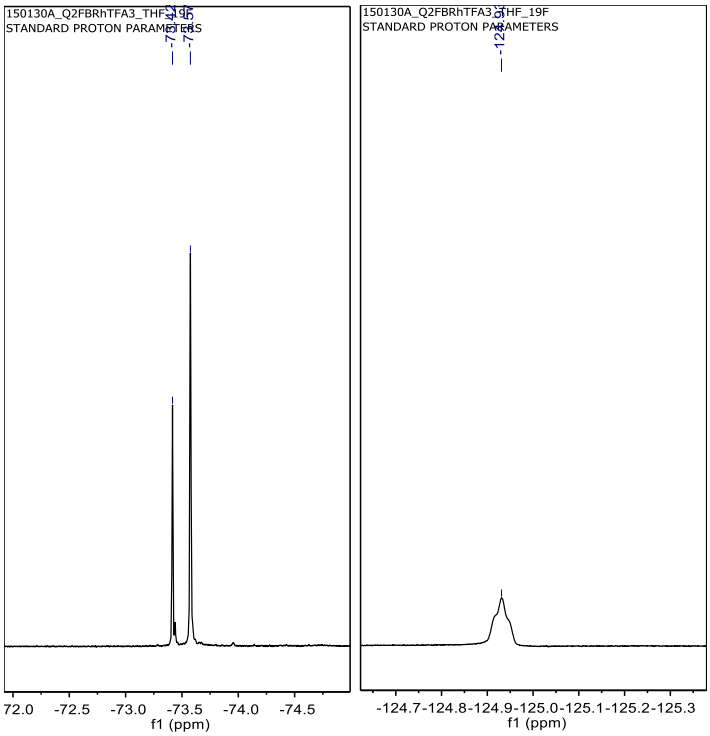

Figure S17. Expanded ^{19}F NMR spectrum (600 MHz, d_8-THF) of **1** $(Q_2FB)Rh(TFA)_3$.

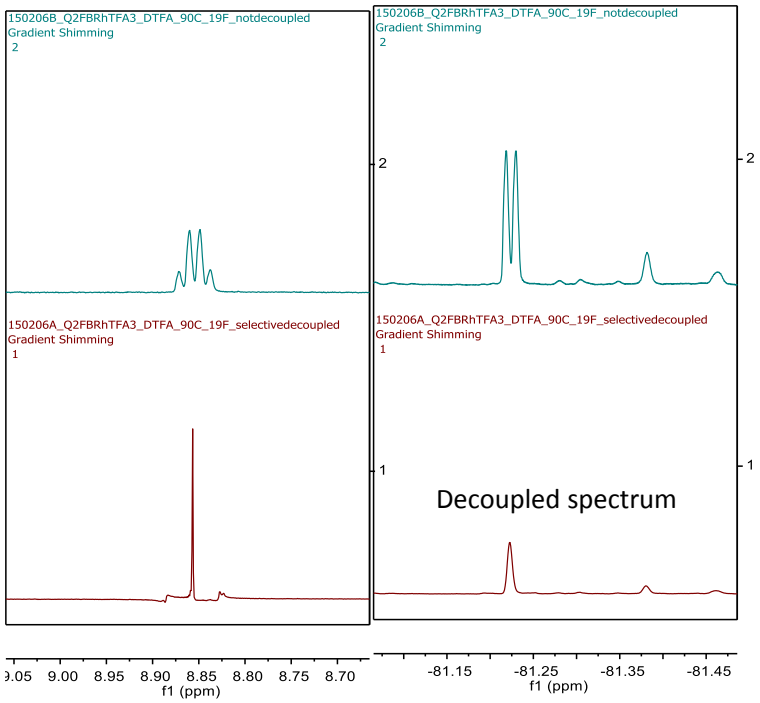

Figure S18. Expanded ^{19}F NMR spectrum (600 MHz, DTFA) of $CF_3C(O)F$ after heating **1** at 90 °C overnight (top), and selectively decoupled spectrum at 8.85 ppm (bottom).

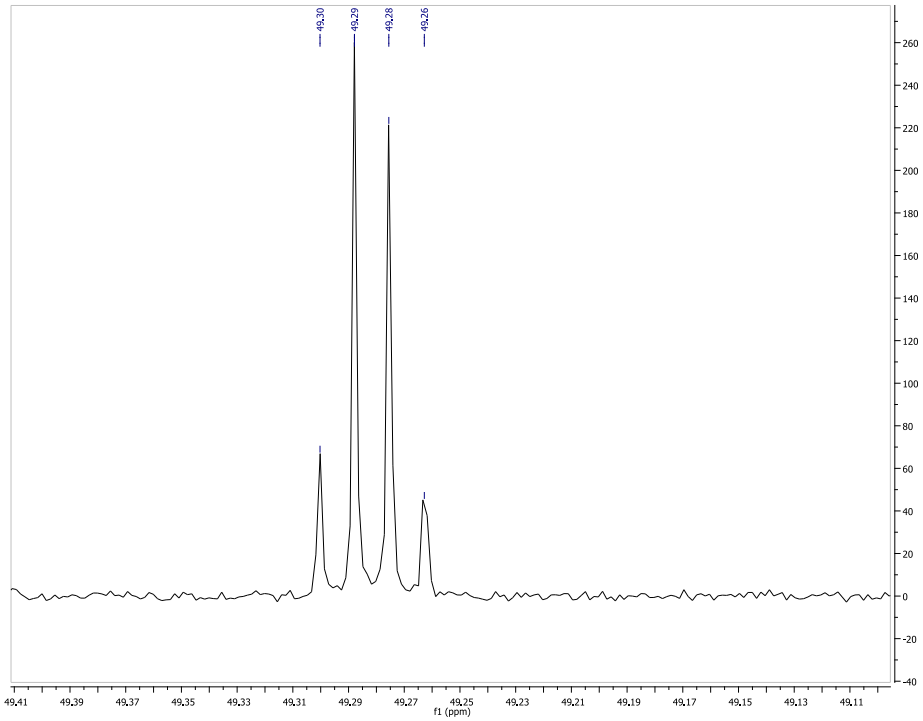

Figure S19. Expanded ^{19}F NMR spectrum (600 MHz) of $CH_3C(O)F$ after heating **1** at 90 °C for 3h.

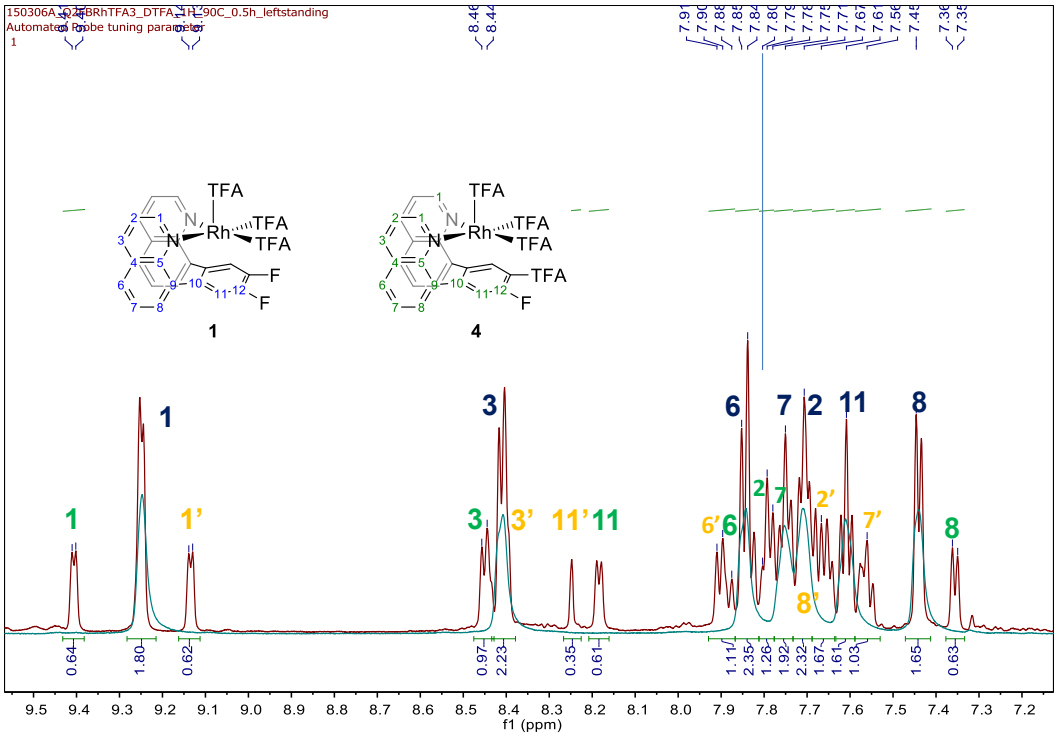

Figure S20. ^{1}H NMR spectra (600 MHz, DTFA). Red spectrum: mixture of **1** (blue labels) and **4** (green and yellow labels). Blue spectrum: reference spectrum of **1**.

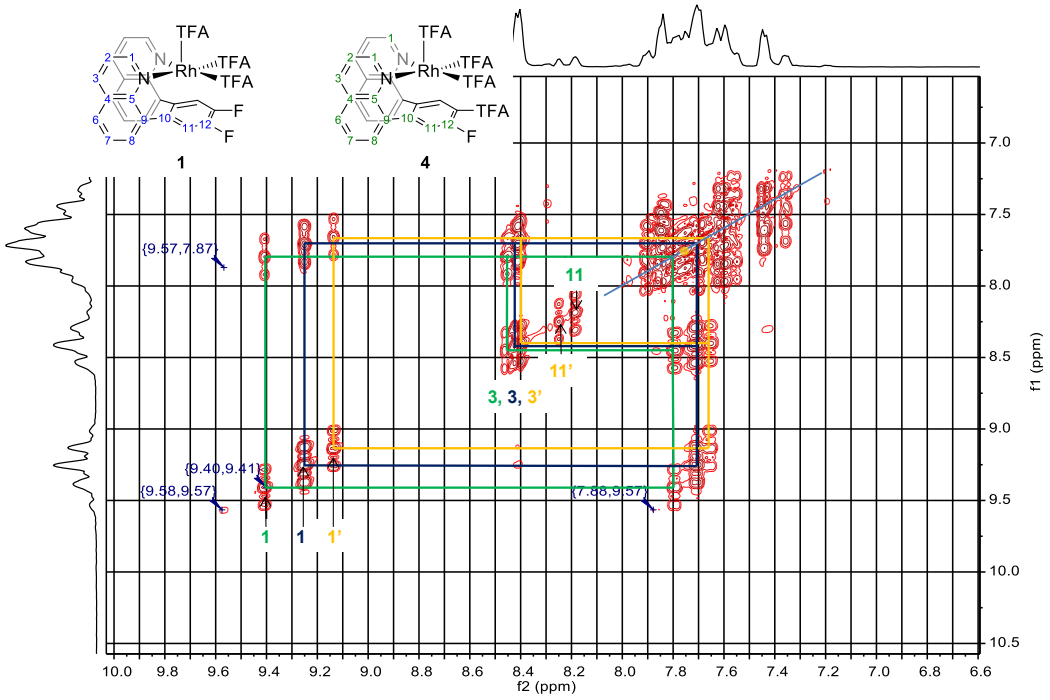

Figure S21. ^{1}H-^{1}H gCOSY NMR spectrum (600 MHz, DTFA) of **1** (blue labels) and **4** (green and yellow labels).

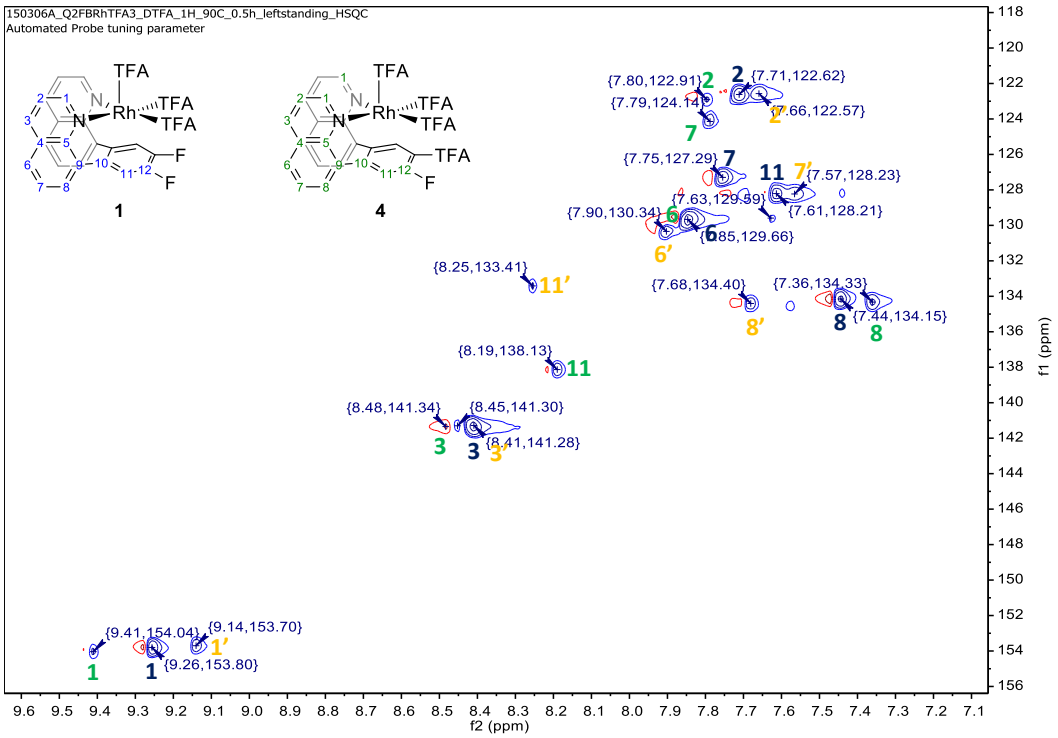

Figure S22. ^{1}H-^{13}C gHSQCAD NMR spectrum (600 MHz, DTFA) of **1** (blue labels) and **4** (green and yellow labels).

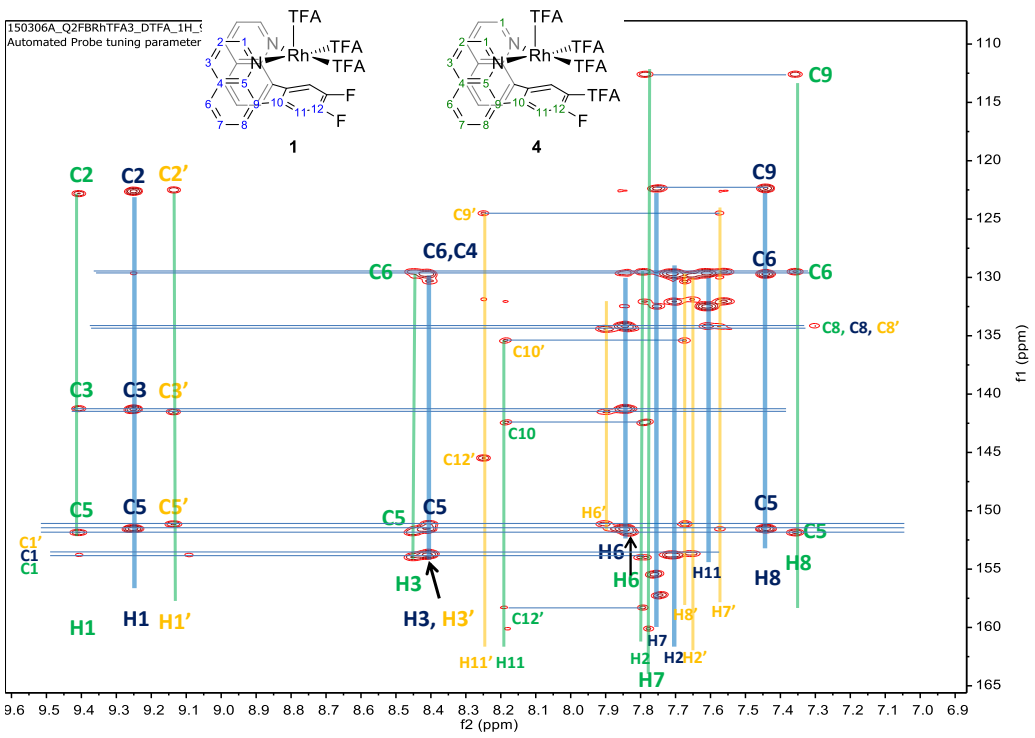

Figure S23. ^{1}H-^{13}C gHMBCAD NMR spectrum (600 MHz, DTFA) of **1** (blue labels) and **4** (green and yellow labels).

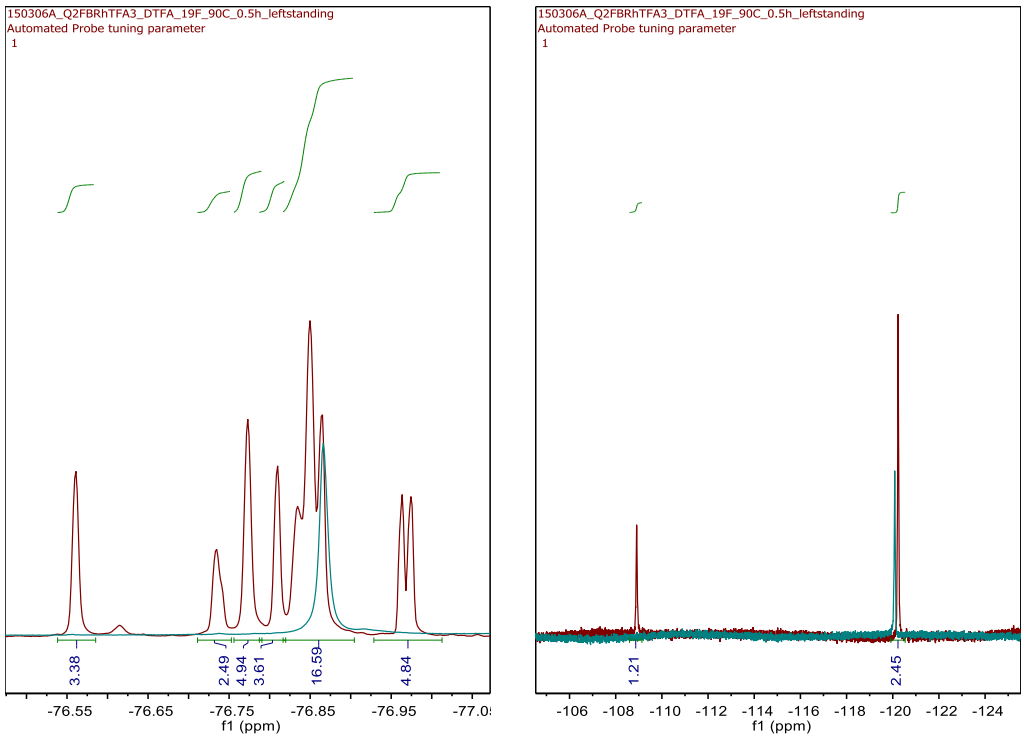

Figure S24. ^{19}F NMR spectra (600 MHz, DTFA). Red spectrum: mixture of **1** (blue labels) and **4** (green and yellow labels). Blue spectrum: reference spectrum of **1**.

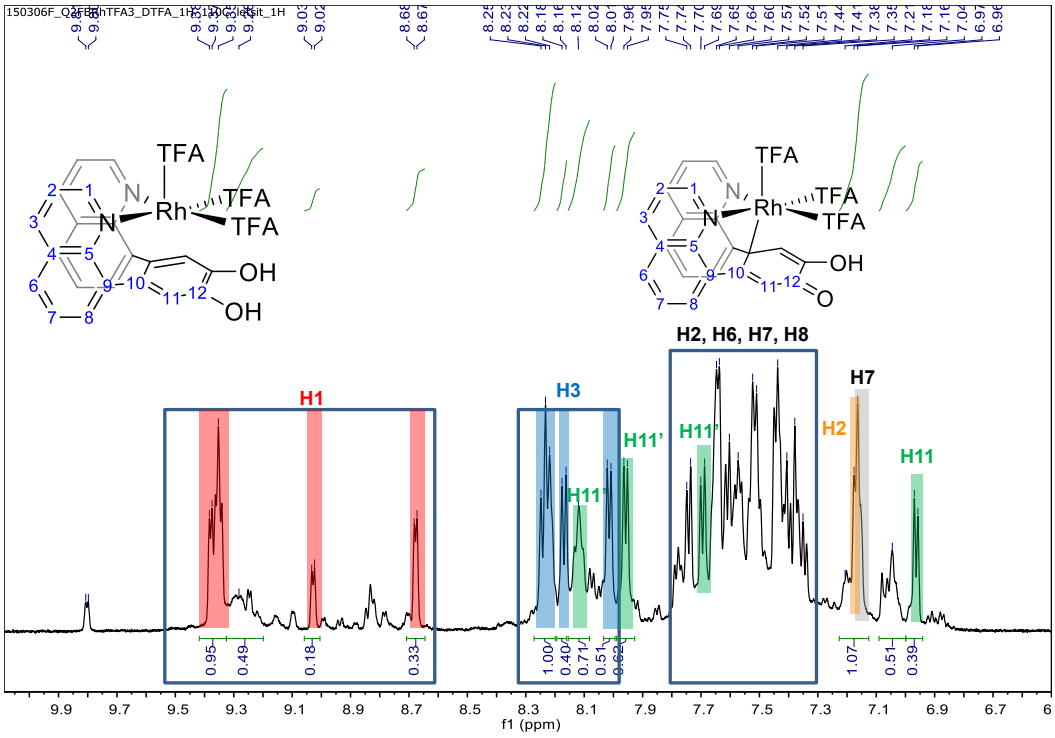

Figure S25. ^{1}H-^{13}C gHSQC NMR spectrum (600 MHz, DTFA) of the proposed **5a** and **5b** from defluorination from **1**.

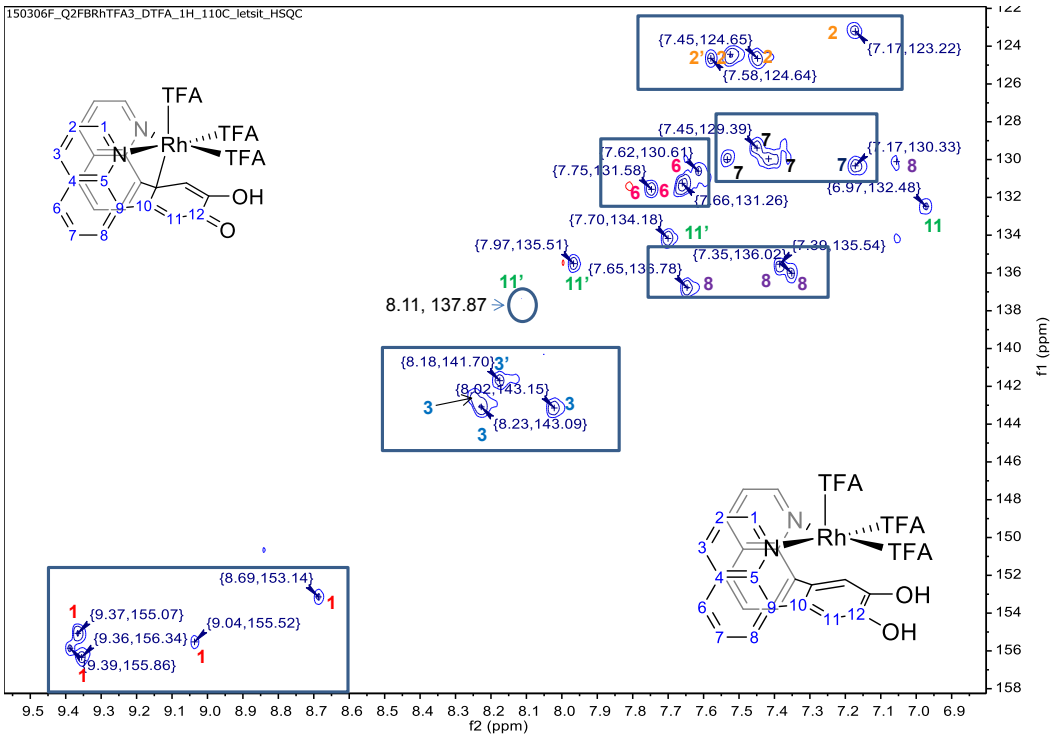

Figure S26. ^{1}H-^{13}C gHSQC NMR spectrum (600 MHz, DTFA) of the proposed **5a** and **5b** from defluorination from **1**.

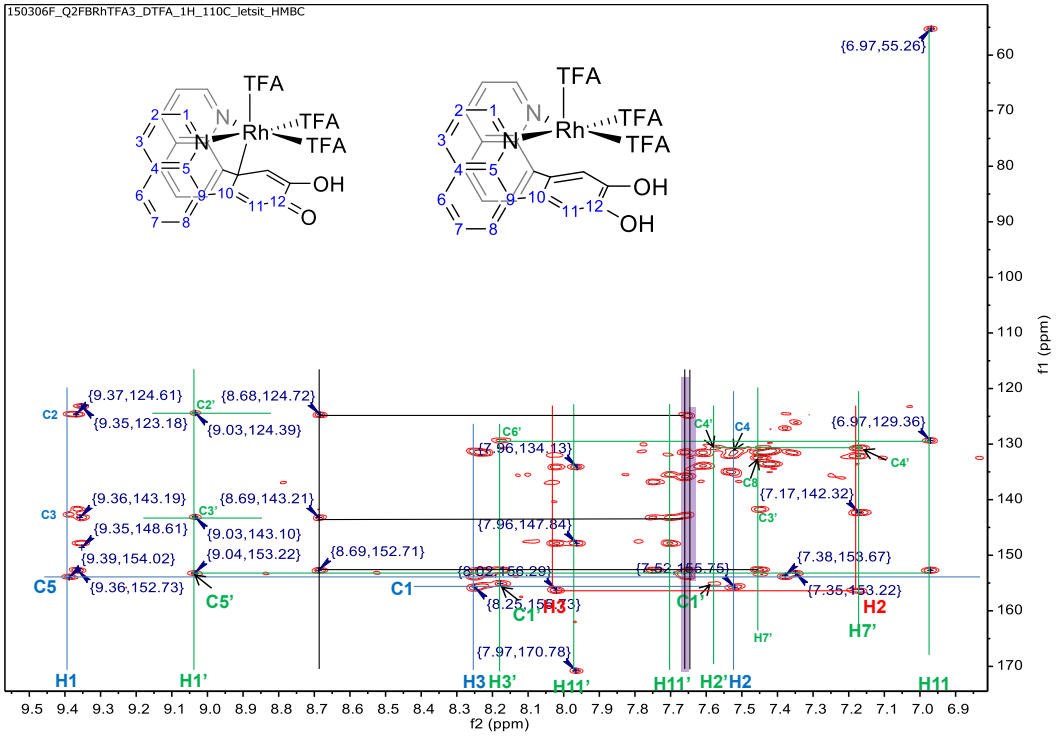

Figure S27. ^{1}H-^{13}C gHMBCAD NMR spectrum (600 MHz, DTFA) of the proposed **5a** and **5b** from defluorination from **1**.

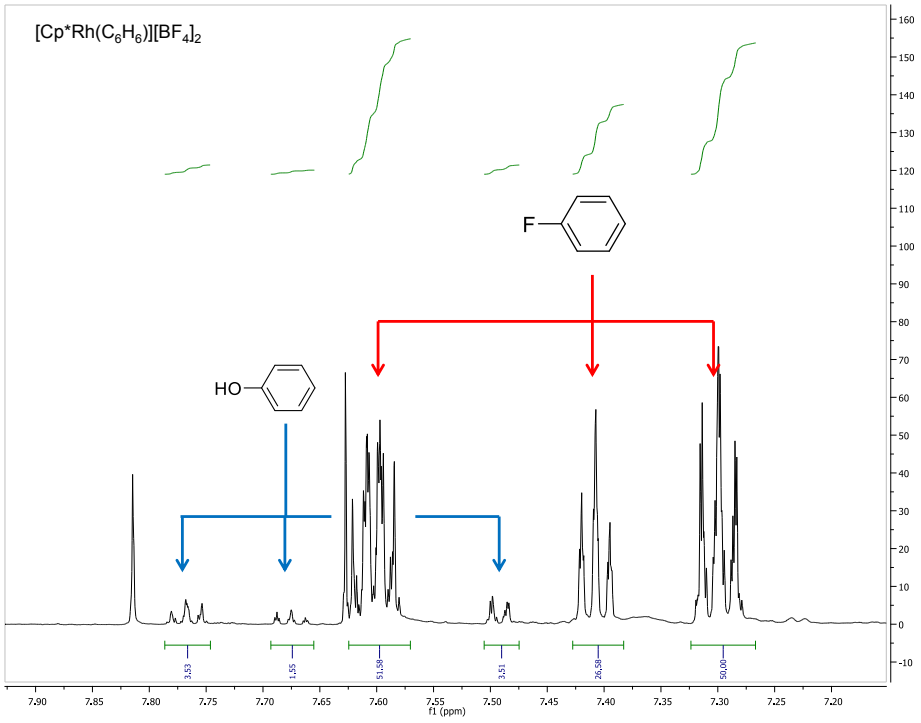

Figure S28. ^{1}H NMR spectrum of catalytic defluorination of fluorobenzene using $[Cp^{*}Rh(C_6H_6)][BF_4]_2$.

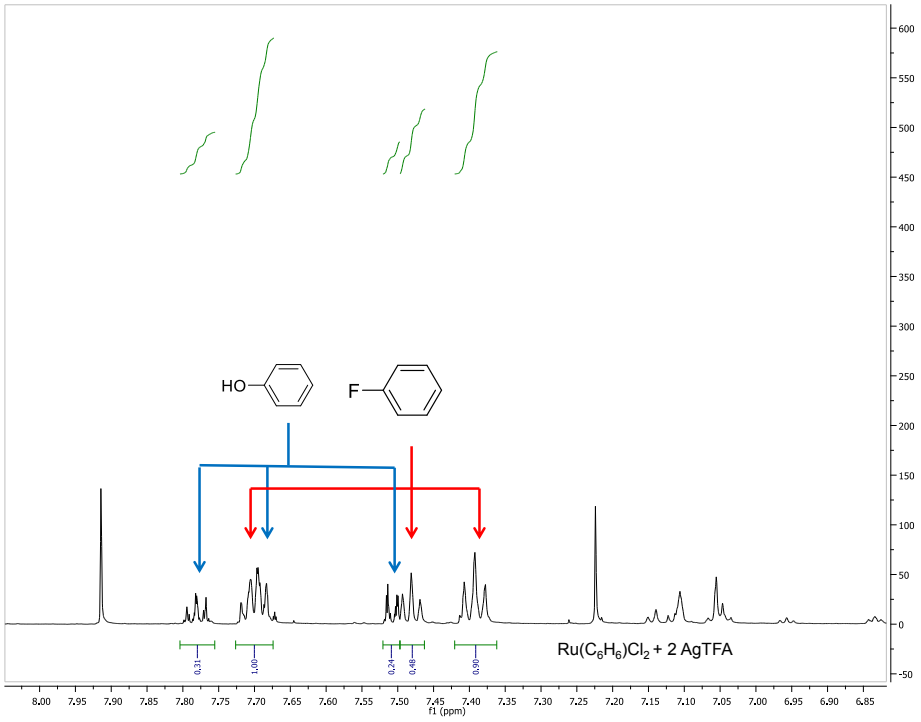

Figure S29. ^{1}H NMR spectrum of catalytic defluorination of fluorobenzene using $Ru(C_6H_6)Cl_2$/AgTFA.

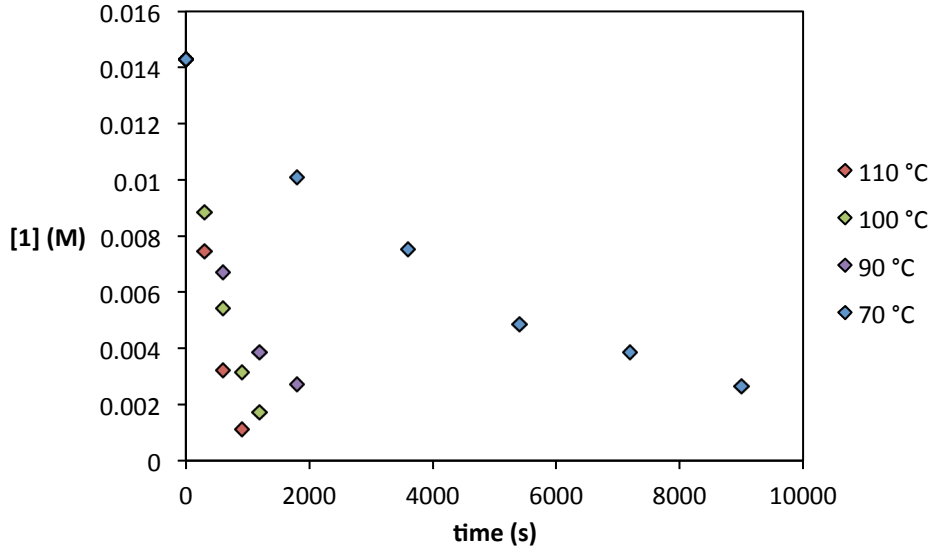

Figure S30. [**1**] vs time for the defluorination of **1** in HTFA.

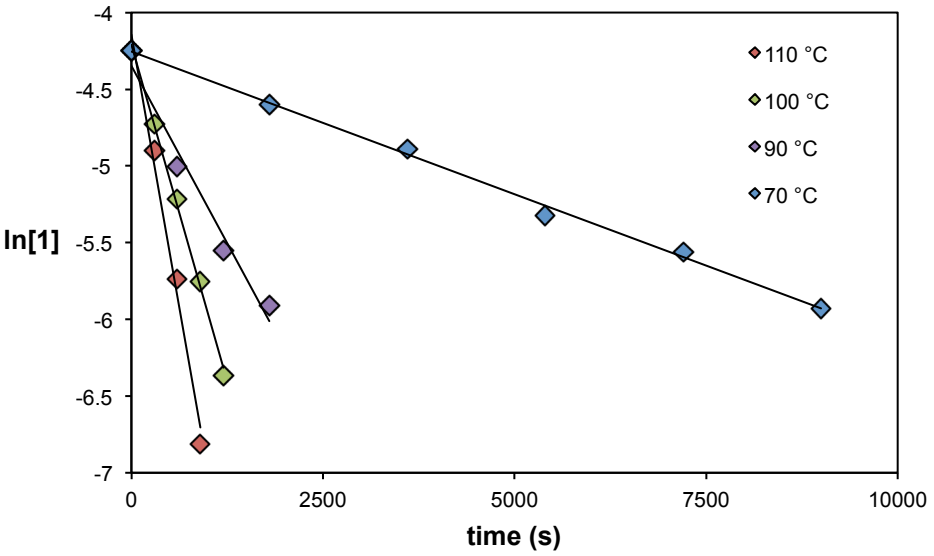

Figure S31. Plot of ln[**1**] vs time for the defluorination of **1** in HTFA.

Table S2. Data for for the defluorination of **1** in HTFA.

T (°C)	70	90	100	110
T (K)	343.15	363.15	373.15	383.15
1/T	0.002914177	0.00275368	0.002679887	0.00261
k	0.00018602	0.00092448	0.001754388	0.002845
(k/T)	5.42096E-07	2.5457E-06	4.70156E-06	7.43E-06
ln(k/T)	-14.4278219	-12.881096	-12.2676154	-11.8105

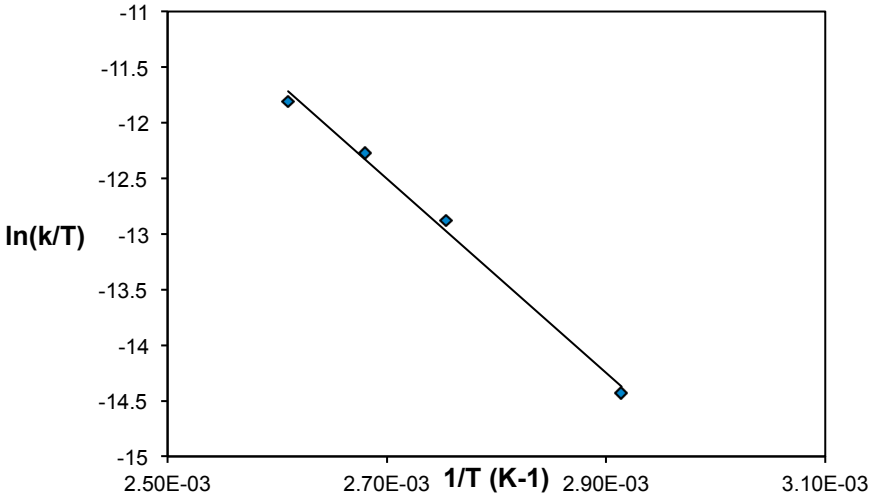

Figure S32. Plot of ln(k/T) vs. 1/T for the defluorination of **1** in HTFA.

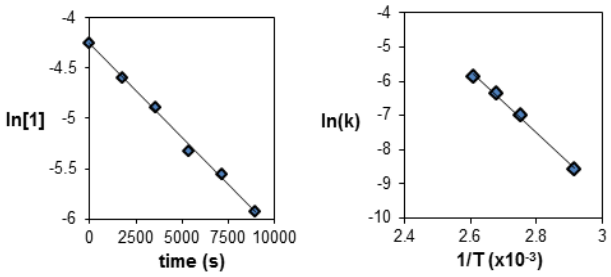

Figure S33. Plot of ln[**1**] vs time (left, 70 °C) and Arrhenius plot (right, 70-110 °C) for decay of **1** during defluorination reaction in HTFA.

Scheme S1. General schematic for S_NAr reactions of fluoroarenes featuring electron-withdrawing groups (EWG).

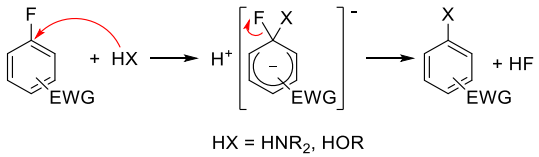

References

(1) Case, F. H. *J. Org. Chem.* **1962**, *27*, 640.
(2) Giordano, G.; Crabtree, R. H. *Inorg. Synth.* **1990**, *28*, 88.
(3) Cramer, R. *Inorg. Synth.* **1990**, *28*, 86.
(4) Frisch, M. J. et al. Gaussian 09, Gaussian, Inc., Wallingford, CT, 2009.
(5) Cossi, M.; Barone, V.; Mennucci, B.; Tomasi, J. *Chem. Phys. Lett.* **1998**, *286*, 253.
(6) Cossi, M.; Rega, N.; Scalmani, G.; Barone, V. *J. Comput. Chem.* **2003**, *24*, 669.
(7) Becke, A. D. *J. Chem. Phys.* **1993**, *98*, 1372.
(8) Becke, A. D. *J. Chem. Phys.* **1993**, *98*, 5648.
(9) Cundari, T. R.; Stevens, W. J. *J. Chem. Phys.* **1993**, *98*, 5555.
(10) Stevens, W. J.; Basch, H.; Krauss, M. *J. Chem. Phys.* **1984**, *81*, 6026.

Computational Methods

Density functional theory (DFT) calculations were used as a supplement to experimental methods to elucidate the defluorination mechanism. For all intermediate states, geometry optimization, frequency, and solvation calculations used the B3LYP functional[1] with a 6-311G** basis set on organic atoms.[2] For rhodium, the Los Alamos small core potential was used[3] alongside a 2-ζ basis set. For single point calculation of electronic energies, the M06 functional was used[4] with the 6-311G**++ basis set on organics.[5] For rhodium, the 3-ζ LACV3P**++ basis set was used with augmented f-functions and diffuse functions. Continuum solvation by trifluoroacetic acid (HTFA) was applied via the Poisson-Boltzmann polarizable continuum model, with a dielectric constant and probe radius of 8.55 and 2.451 Å, respectively. In cases where solvent participated in the reaction or stabilized a transition state, explicit solvent was used. Transition states were also calculated in this analysis and were verified by the presence of negative frequencies.

In order to report free energies (G), the following equation was used:

$$G = E_{M06} + G_{solv} + E_{ZPE} + H_{vib} + H_{TR} - T(S_{vib} + S_{elec})$$

where E_{M06} is the electronic energy taken from the single point energy calculation, G_{solv} is the energy of solvation, and E_{ZPE} is the zero point energy correction taken from frequency calculations. H_{vib} and H_{TR} are the vibrational and translational/rotational enthalpies ($^{12}/_{2}k_BT$), respectively. S_{vib} and S_{elec} are the vibrational and electronic entropy contributions to the free energies. All enthalpic and entropic values are taken from frequency calculations. For NMR simulations, B3LYP and large basis sets were used with implicit solvation to calculate species of interest and the standard, trimethylsilane (TMS). All calculations are completed in Jaguar[6] and have been shown previously to agree with experiment.[7]

References

(1) (a) Becke, A. D. *J. Chem. Phys.* **1993**, *98*, 5648(b) Lee, C. T.; Yang, W. T.; Parr, R. G. *Phys. Rev. B* **1988**, *37*, 785.

(2) Hehre, W. J.; Ditchfie.R; Pople, J. A. *J. Chem. Phys.* **1972**, *56*, 2257.

(3) Hay, P. J.; Wadt, W. R. *J. Chem. Phys.* **1985**, *82*, 299.

(4) Zhao, Y.; Truhlar, D. G. *Theor. Chem. Acc.* **2008**, *120*, 215.

(5) (a) Krishnan, R.; Binkley, J. S.; Seeger, R.; Pople, J. A. *J. Chem. Phys.* **1980**, *72*, 650(b) Clark, T.; Chandrasekhar, J.; Spitznagel, G. W.; Schleyer, P. V. *J. Comp. Chem.* **1983**, *4*, 294.

(6) Bochevarov, A. D.; Harder, E.; Hughes, T. F.; Greenwood, J. R.; Braden, D. A.; Philipp, D. M.; Rinaldo, D.; Halls, M. D.; Zhang, J.; Friesner, R. A. *Int. J. Quantum Chem.* **2013**, *113*, 2110.

(7) (a) Zhao, Y.; Truhlar, D. G. *J. Chem. Theory Comp.* **2009**, *5*, 324(b) Young, K. J. H.; Lokare, K. S.; Leung, C. H.; Cheng, M.-J.; Nielsen, R. J.; Petasis, N. A.; Goddard Iii, W. A.; Periana, R. A. *J. Mol. Cat. A: Chem.* **2011**, *339*, 17(c) O'Reilly, M. E.; Fu, R.; Nielsen, R. J.; Sabat, M.; Goddard, W. A.; Gunnoe, T. B. *J. Am. Chem. Soc.* **2014**, *136*, 14690.

NMR Simulations via DFT

In order to aid in the assignment of **5a** and **5b**, NMR calculations were carried out via DFT. Experimentally, several of the carbons had shifts that were slightly higher than expected. To calibrate our calculations, we first calculated the shifts on relevant carbons for the well-characterized complex **1.** As seen in table S3, the error between experimental and calculated shifts is 5-10 ppm. While this error does not allow for quantitative comparisons, qualitative trends may be seen.

Table S3. Experimental and calculated shifts are compared. The two carbons in the calculated complex are averaged, since the complex is symmetrical.

Carbon	Experimental	Calculated	Difference
8	134.9	128.0	6.9
9	123.0	129.2	-6.2
10	134.4	124.3	10.1
11	127.9	128.4	-0.5
12	156.0	162.1	-6.1

In the case of **5a**, we see that OH can orient itself to the Rh-bound TFA in two ways (Figure S44): first with the O on TFA and the other with one of the F atoms on TFA. When this occurs, the symmetry of the complex is broken and a corresponding asymmetry is seen in the ^{13}C shifts. Since both hydroxyl groups can orient in this manner, this likely increases the shift, as seen in Table S4. Furthermore, the proton from the hydroxyl groups can transfer to the coordinated TFA to form species **5b**. Again, asymmetry in the ^{13}C shift is seen in Table S5. Explicit solvent can also loosely coordinate through hydrogen bonding, also seen in Table S5. This also increases the ^{13}C shift, though perhaps not significantly.

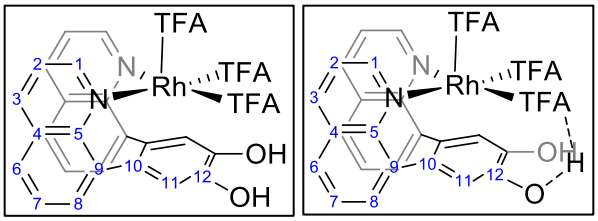

Figure S34. Proposed geometries of complex **5a**. In the geometry on the left, a perfectly symmetric complex is proposed. However, on the right, it is implied that coordination between either the O or F of TFA can occur. This corresponds to values in Table S4.

Table S4. Experimental and calculated shifts for complexes in Figure S44.

Atom	Exp. Shift	Atom	Calc. Shift H--O	Calc. Shift H--F
8	148.3	**8 O Rotated**	127.8	130.0
8	148.3	**8 O**	128.8	130.8
9	143.8	**9 O Rotated**	131.2	135.6
9	143.8	**9 O**	134.7	133.7
10	129.7	**10 O**	161.0	160.1
10	129.7	**10 O Rotated**	87.1	87.5
		10 avg	124.1	123.8
11	127.9	**11 O**	117.2	144.2
11	127.9	**11 O Rotated**	148.0	115.9
12	136	**12 O**	175.9	147.2
12	136	**12 O Rotated**	149.6	171.0

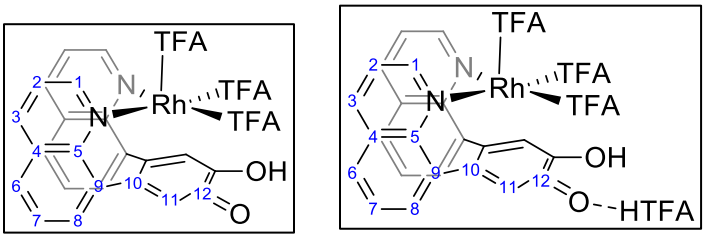

Figure S35. Complex **5b** without (left) and with (right) coordinated solvent.

Table S5. Shifts seen in **5b**, both with and without coordinated solvent.

Atom	Exp. Shift	Atom	No Coordinated Solvent	Coordinated Solvent
8	148.3	**8 O**	130.5	136.4
8	148.3	**8 OH**	133.6	132.6
9	143.8	**9 O**	137.5	137.9
9	143.8	**9 OH**	144.3	141.3
10	129.7	**10 O**	174.3	176.7
10	129.7	**10 OH**	73.2	72.1
		10 (avg)	123.8	127.4
11	127.9	**11 O**	130.1	128.6
11	127.9	**11 OH**	136.0	139.7

12	136	**12 O**	191.8	189.5
12	136	**12 OH**	157.4	153.5

It can be suggested that the increased experimental shifts result from a combination of asymmetric coordination and solvent coordination. Asymmetry in the molecule is translated to the asymmetric shifts, which averages to a slightly higher shift overall. Additionally, as suggested by DFT energy calculations, there is potentially equilibrium between **5a** and **5b**, as the proton can quickly hop around from the ring to the TFA molecules. This, in combination with the solvent participation, can increase the overall experimental shifts.

Scheme S2. Proposed mechanism for the defluorination of 1.

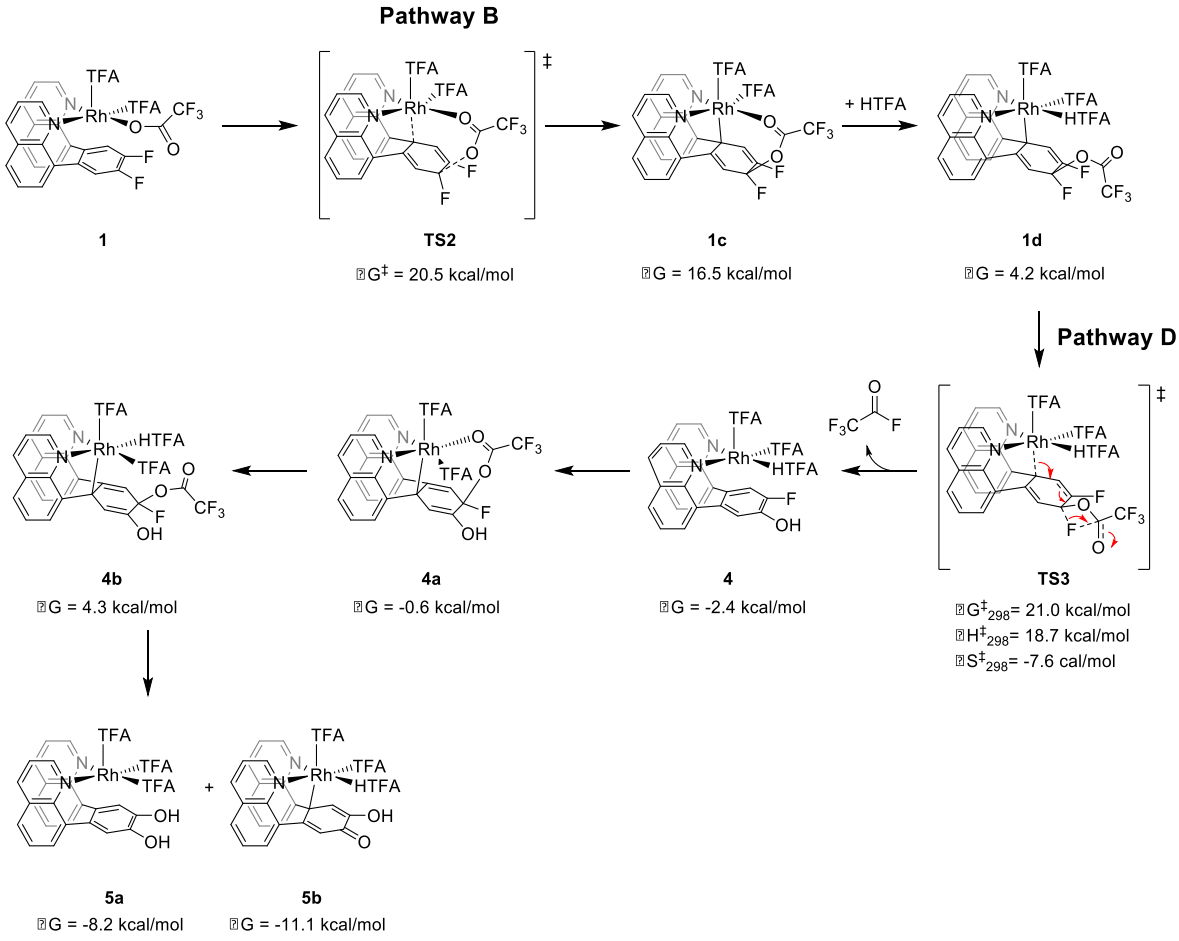

Accounting for Solvation in Transition States

In **TS1** and **TS3**, explicit solvent was used. In the case of **TS1**, two solvent molecules were chosen on a purely geometric basis: two solvent molecules were the minimum number of molecules required to bridge between the metal-bound TFA and the TFAH binding to aryl group. In the case of **TS3**, one solvent molecule was used. In order to account for the multiple degrees of freedom that come with incorporating an explicit molecule, we have investigated several different isomers of **TS3**, which can be seen in Scheme **S2**. **TS3b** involves a TFAH with its hydrogen oriented towards the oxygen of the bound TFA. This increases the energy by 4.1 kcal/mol relative to the reported **TS3**. **TS3c** is attack from the fluorine above the ring (closer to the Rh), with a TFAH oriented towards it via the proton. This is also higher in energy, both due to the increased electronic energy and the added strain from fitting an explicit TFAH into the cavity. Finally, **TS3d** involves fluorine bridging with no added TFAH, which is again higher in energy by 5.2 kcal/mol, showing that the free TFAH does help to stabilize the transition state. While this does not exaust all possibilities for the role of TFAH, it does help to illustrate that a specific orientation (TFAH with hydrogen pointed towards the fluorine) helps to stabilize the transition state and make it more accessible.

Scheme S3. Alternatives to TS3

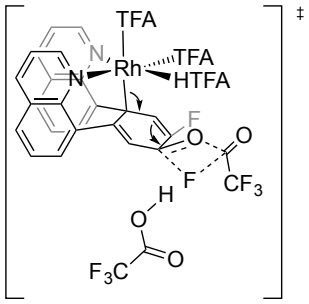

TS3 (reported)
ΔG = 21.0

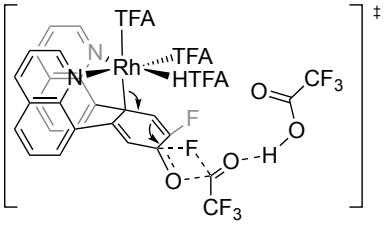

TS 3b
ΔG = 25.1

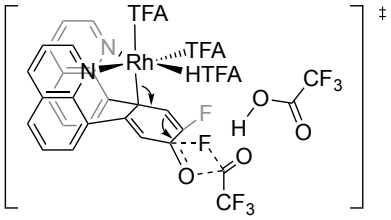

TS 3c
ΔG = 27.6

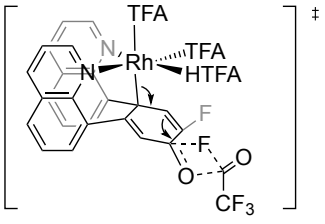

TS 3d (no explicit solvent)
ΔG = 26.2

Geometries- "The supplemental file Fluoro_Coord.xyz contains the computed Cartesian coordinates of all of the molecules reported in this study. The file may be opened as a text file to read the coordinates, or opened directly by a molecular modeling program such as Mercury (version 3.3 or later, http://www.ccdc.cam.ac.uk/pages/Home.aspx) for visualization and analysis.

Table S6. Table of DFT Values

Molecule	ZPE (kcal/mol)	H_{vib}	S_{vib}	6kT	½ (S_{trans} + S_{cis})	Selec	H_{tot}	S_{tot}	G(solv) - sTFA	E(LB, M06)	G(TFA)	H	# basis
1	254.8	24.7	173.1	3.6	42.2	0.0	27.1	256.2	-0.03447	-2919.69729	-1831941.84	-1831876.6	1226
Mol 1b1 exp solv.				3.6							3.47	3.6	
Mol 1b2 exp solv.	280.1	29.6	2106	3.6	42.8	0.0	32.0	296.7	-0.02825	-3446.46921	-2162473.60	-2162397.0	1387
Mol 1b2 2 exp solv.	305.4	34.7	250.5	3.6	43.4	0.0	37.1	340.3	-0.03029	-3973.24596	-2492014.00	-2492925.3	1548
1_2a	263.0	26.7	173.2	3.6	42.2	0.0	26.7	249.8	-0.07201	-2920.08623	-1832184.05	-1832118.8	1233
1_2b	262.8	24.5	170.1	3.6	42.2	0.0	26.9	253.7	-0.05578	-2920.08623	-1832190.57	-1832126.2	1219
1_2c				3.6								3.6	
1c	255.3	24.7	165.5	3.6	42.2	0.0	27.0	254.9	-0.03023	-2919.67982	-1831925.56	-1831862.6	1226
1b	281.1	29.0	204.6	3.6	42.9	0.0	31.3	292.0	-0.02545	-3446.47652	-2162474.29	-2162399.4	1387
4	263.0	25.2	171.1	3.6	42.2	0.0	27.6	259.6	-0.03335	-2895.69085	-1816867.70	-1816803.0	1233
5a	271.1	25.2	170.7	3.6	42.2	0.0	27.5	258.5	-0.03368	-2871.68673	-1801796.86	-1801732.3	1240
5b	271.0	24.7	172.5	3.6	42.2	0.0	27.1	258.1	-0.03111	-2871.69218	-1801799.73	1801734.7	1240
10c	281.1	29.2	205.5	3.6	42.8	0.0	31.5	293.6	-0.01795	-3446.45256	-2162454.62	-2162379.5	1387
1d	280.6	28.8	201.0	3.6	42.9	0.0	31.2	284.4	-0.02592	-3446.48013	-2162476.45	-2162402.7	1387
TS3	303.1	33.4	242.8	3.6	43.5	0.0	35.8	325.9	-0.03041	-3973.21025	-2492993.03	-2492906.6	1548
TS2	254.3	24.6	165.8	3.6	42.2	0.0	27.0	255.9	-0.03246	-2919.66915	-1831921.32	-1831858.3	1226
TS1	329.6	38.0	277.0	3.6	43.9	0.0	40.4	361.5	-0.03115	-4499.98009	-2823525.85	-2823429.1	1709
1d with HF	286.7	31.1	217.1	3.6	42.8	0.0	33.5	308.4	-0.07242	-3446.83607	-2162725.33	-2162646.8	1394
1d with HF, neutral	278.6	30.2	215.4	3.6	42.8	0.0	32.6	302.2	-0.03974	-3446.45603	-2162474.78	-2162396.7	1387
TS4 (Free F)	302.9	33.6	242.8	3.6	43.4	0.0	35.9	326.6	-0.03783	-3973.16268	-2492967.81	-2492881.4	1548
Small Molecules													
HTFA	24.6	2.1	14.0	3.6	33.7	0.0	4.5	81.3		-526.75300	-330538.77	-330514.5	161
$CF_3C(O)F$	16.6						4.4	80.3	0.0	-550.8	-345589.5	-345589.5	154
H^+	-266.2												

Molecules	ΔG	ΔH	Molecules	ΔG	ΔH	Molecules	ΔG	ΔH
1c	16.3	14.0	**10c**	26.0	11.6	**TS4 w/ HTFA**	46.2	43.9
1b	6.3	-8.3	**TS2**	20.5	18.3			
4	-2.4	-1.4	**TS1**	26.9	10.8			
1d	4.2	-11.5	**TS3**	21.0	18.7			
5a	-8.2	-5.7	**1d with HF**	21.5	10.6			
5b	-11.1	-8.0	**1d with HF, neutral**	5.8	-5.6			